



# Cultivar governs plant response to inoculation with single isolates and the microbiome associated with arbuscular mycorrhizal fungi

Cristina Rotoni<sup>a,b</sup>, Marcio F.A. Leite<sup>a</sup>, Lina C. Wong<sup>a</sup>, Cátia S.D. Pinto<sup>a</sup>, Sidney L. Stürmer<sup>c</sup>, Agata Pijl<sup>a</sup>, Eiko E. Kuramae<sup>a,b,\*</sup>

<sup>a</sup> Netherlands Institute of Ecology (NIOO-KNAW), Droevendaalsesteeg 10, 6708 PB Wageningen, the Netherlands

<sup>b</sup> Ecology and Biodiversity, Institute of Environmental Biology, Utrecht University, Padualaan 8, 10 3584 CH Utrecht, the Netherlands

<sup>c</sup> Departamento de Ciências Naturais, Universidade Regional de Blumenau, Blumenau, SC 89030-903, Brazil

## ARTICLE INFO

### Keywords:

Bacterial community  
Fungal community  
Siderophore  
Indole-3-acetic acid  
Phosphate solubilization  
*Acaulospora morrowiae*  
*Claroideoglomus etunicatum*  
*Rhizophagus clarus*  
*Funelliformis* sp.  
*Glomus* sp1 and *Glomus* sp2  
Generalized joint attribute model

## ABSTRACT

Plant Growth-Promoting Microbes (PGPM) have the potential to enhance sustainable agriculture, but there is still a limited understanding of how the complex interplay between plant genetic variability, the native soil community, and soil nutrients affects PGPM recruitment. To address this challenge, we investigated the impact of bacteria isolates and arbuscular mycorrhizal fungi (AMF) along with their accompany microbiome (AMFc) derived from a wild chrysanthemum on the growth of five different commercial chrysanthemum cultivars (Chic, Chic 45, Chic Cream, Haydar and Barolo), as well as their rhizosphere microbiomes, within a nutrient-rich complex substrate environment. We found 23 bacterial strains capable of producing siderophore, 14 strains capable of producing Indole-3-acetic acid, and 18 strains capable of solubilizing phosphate. The AMFc had six AMF species, and the bacterial and fungal communities associated with AMF belonged to different phyla. Using generalized joint models, we investigated the impact of the three most effective bacterial strains and the AMFc on plant growth (shoot and root dry mass) while integrating information on plant genotype, environment, and microbes. The impact of PGPM inoculation varied from positive to negative effects depending on the cultivar, with Chic Cream showing the highest increase in root biomass after inoculation with both bacterial strain SMF006 (57 %) and AMFc inoculation (79 %). Our study demonstrates that PGPM from wild relative can impact the growth and assembly of the chrysanthemum root microbiome, but this impact is cultivar-dependent. Furthermore, inoculation with a complex AMF containing community (AMFc) induced greater changes in the rhizosphere microbiome than with a single bacterial isolate. Our study shows that inoculation of a complex community of beneficial microbes results in more effective plant growth promotion.

## 1. Introduction

The use of beneficial microorganisms to promote plant growth and health, known Plant Growth-Promoting Microbes (PGPM), is a promising alternative to reduce the dependence on inorganic fertilizers leading to more sustainable agriculture (Basu et al., 2021; Liu et al., 2022; Naamala and Smith, 2020), but their effective usage faces many challenges. First, inoculation of either single or more complex communities of PGPM in living soil may result in diminished effect because of the native soil community resistance and resilience, thus compromising the efficiency of the applied PGPM (Armada et al., 2018). Second, even when the inoculated PGPM manages to reach and access the plant, its efficiency is also not guaranteed since beneficial interactions between

plants and microbes may have been lost during plant domestication, which could be attributed to agricultural practices such as plant breeding, fertilizer use, and pesticide application (Chang et al., 2021b, 2022). Therefore, the effective use of PGPM, such as bacteria and arbuscular mycorrhizal fungi (AMF) largely depends on the host preference and the already established soil community.

However, the adoption of PGPM further increases the already high complexity of plant-microbe interactions in the rhizosphere. As a result, researchers have adopted to study simplified versions of this system based on two criteria: sterilized environment and/or focus on one specific plant growth promotion trait. First, in an attempt to detect the direct effect of PGPM, studies are often conducted in sterile soils and under controlled environmental conditions. Second, the adoption of

\* Corresponding author at: Netherlands Institute of Ecology (NIOO-KNAW), Droevendaalsesteeg 10, 6708 PB Wageningen, the Netherlands.

E-mail address: [e.kuramae@nioo.knaw.nl](mailto:e.kuramae@nioo.knaw.nl) (E.E. Kuramae).

<https://doi.org/10.1016/j.apsoil.2024.105347>

Received 19 October 2023; Received in revised form 13 February 2024; Accepted 20 February 2024

Available online 1 March 2024

0929-1393/© 2024 The Authors. Published by Elsevier B.V. This is an open access article under the CC BY license (<http://creativecommons.org/licenses/by/4.0/>).

PGPM often focus on a small number of well-characterized microbes or specific plant growth promotion traits. Consequently, the selection of promising PGPM runs the risk of failing when transferred to complex field conditions (Parnell et al., 2016). To increase the efficiency of PGPM, we need to understand the interactions that shape the phenotype of the plant host by disentangling the relative contribution of (i) plant genotype, (ii) the environment, and (iii) the microbiome (Chang et al., 2021a; Oyserman et al., 2021). We are aware that the nutrient input reshape how plants recruit PGPM and may even reduce their contribution to plant growth and nutrient acquisition (Leite et al., 2017). Additionally, we have gained some understanding of how the native microbiome can exhibit resistance and/or resilience to the inoculation of beneficial microbes (Armada et al., 2018; Wang et al., 2022). Unfortunately, previous studies lacked a quantitative assessment of how the microbiome's impact contributed to the variability in plant response, particularly when the plant genotype is altered during plant breeding. Previous studies have shown that different cultivars selected a unique set of microbes strongly linked to their genetic variability (Abera et al., 2022; Bulgarelli et al., 2022; Chang et al., 2021b; Li et al., 2023; Rotoni et al., 2022; Schlemper et al., 2017) but we still lack more in-depth studies on how this genetic variability influences the response of these plants to the inoculation of beneficial microbes.

In the current study, we employed five chrysanthemum (*Chrysanthemum indicum* L.) cultivars as a plant model system to investigate the potential contributions of plant genotype and the environment in the adoption of PGPM. We tested the following hypotheses: (i) bacteria as well as AMF plus their accompany microbiome (that from now we call AMFc), isolated from wild chrysanthemum impact growth and root microbiome assembly of commercial cultivars of chrysanthemum, and (ii) chrysanthemum genotypes influence the efficiency of PGPM in enhancing plant growth. To test these hypotheses, we first obtained microbial isolates (bacteria and AMFc) from a wild relative of the commercial cultivars of chrysanthemum. Then, we tested the contribution of both bacteria and AMFc in promoting root growth at an early development stage of the cuttings, our desired plant phenotype, when inoculated into an already complex environment: a nutrient-rich substrate with a native soil microbial community. Finally, by taking advantage of joint models (Leite and Kuramae, 2020), we aim to disentangle the tripartite interaction (Genotype x Environment x Microbe) and identify the relative contribution of the inoculated PGPM (bacteria or AMFc) in the root growth of chrysanthemum cuttings. This approach allows to select the best isolates that promote plant growth in already complex environment and different cultivars, thus increasing the chances of successfully transferring the isolates to field conditions.

## 2. Materials and methods

### 2.1. Soil source and isolation of bacterial strains

Bacterial strains were isolated from the rhizosphere, endosphere, and the bulk soil surrounding wild chrysanthemum plants growing in natural grassland in Ede, the Netherlands. The plants were growing in a silty-clay soil with the nutrient composition described in Table S1. The climate of the sampled area is classified as oceanic (Cfb) with an average annual temperature of 10.6 °C and rainfall of 848 mm.

Bacteria from the root endosphere were isolated using a modified method described by Cipriano et al. (2016). First, the exterior portions of the collected roots were washed with sterile tap water, followed by double-distilled sterile water. The root samples were then soaked in 70 % ethanol for 60 s, dipped in 3 % sodium hypochlorite for 3 min, and soaked in 70 % ethanol for an additional 30 s. This process was repeated five times to ensure that the root samples were properly disinfected. Next, the disinfected plant tissue from four representative samples was macerated and ground in a sterile mortar and pestle using sterile phosphate buffer saline (PBS) solution, pH 7.4. The root extracts were then serially diluted ( $10^{-2}$  to  $10^{-4}$ ), and an equal volume (100  $\mu$ l) of

aliquot from each dilution was plated onto Luria-Bertani (LB) agar and Tryptic Soya Agar (TSA) in triplicates.

To isolate bacteria from the rhizosphere, plants were removed from the soil and shake vigorously to remove the soil loosely attached to the roots (Leite et al., 2021). In brief, the soil roots tightly adhered to the roots were placed in a 50 ml tube with a 20 ml buffer of 10 mM MgSO<sub>4</sub>, pH 7.0. The solution was pulsed at 1500  $\times$ g for 1 min. The rhizosphere filtrate was diluted ( $10^{-2}$  to  $10^{-4}$ ) in a sequence, each diluted volume (100  $\mu$ l) was spread in LB agar and in triple TSA media.

To isolate bacteria from the soil, 1 g of dried soil samples was dissolved in 10 ml sterile distilled water. The soil sample was manually shaken vigorously for 2 min and serially diluted in distilled water to  $10^{-4}$ , and 100  $\mu$ l of aliquot was spread on three plates of LB and TSA media.

The plates containing endosphere, rhizosphere, and soil isolations were incubated at 25 °C for two to four days in the dark. The number of colonies appearing on solid media was determined by examining the plates at a magnification of  $\times 10$  with a stereomicroscope. One colony of each bacterium morphology was picked and streaked on fresh TSA medium plates to obtain pure cultures. Purified strains were cryopreserved in 30 % v/v glycerol and stored at  $-80$  °C.

### 2.2. Screening bacterial isolates for plant growth promotion traits and molecular characterization

As plant growth promotion (PGP) traits we checked the isolated bacteria capacity of: siderophore production, phosphate solubilization, and Indole-3-acetic acid (IAA) production. The capacity of the strains to produce siderophore followed the method of Schwyn and Neilands (1987), in which a dye, chromeazuroil S (CAS) forms a dye-iron complex that causes a color change from blue to yellow–orange. The phosphate solubilization assay was performed according to (Nautiyal, 1999). The strains were cultured for 15 days in triplicates on National Botanical Research Institute's phosphate solid growth medium - containing tricalcium phosphate as the insoluble phosphate source, 1 l of NBRIP medium contained 10 g of D-glucose, 5 g of Ca<sub>3</sub>(PO<sub>4</sub>)<sub>2</sub>, 5 g of MgCl<sub>2</sub> \* 6 H<sub>2</sub>O, 0.25 g of MgSO<sub>4</sub> \* 7 H<sub>2</sub>O, 0.2 g of KCl and 0.1 g of (NH<sub>4</sub>)<sub>2</sub>SO<sub>4</sub>, 1.5 g of Agar, in demineralised water, pH 7.0. The ability of the bacteria to solubilize calcium phosphate was verified by the formation of a clear halo surrounding the colonies. For the IAA production, the precursor of IAA (Bric et al., 1991), L-tryptophan (1 g/l), was added to a Luria Bertani (LB) liquid medium and incubated with shake at 28 °C in the dark for 72 h. Culture supernatants from each of these isolates were mixed with Salkowski reagent (50 ml, 35 % of perchloric acid, 1 ml 0.5 M FeCl<sub>3</sub> solution) in the ratio of 1:1. Development of pink color indicates the production of IAA, and its optical density was recorded at 540 nm. The concentration of the IAA produced was estimated against the standard curve of IAA in the range of 10–100  $\mu$ g/ml.

A descriptive qualitative scale was used for PGP production traits based on the area of color change on the plate, shifting from blue to green or yellow (for siderophores), the formation of a clear halo surrounding the colonies (phosphate solubilization), and the development of a pink color, along with recording optical density at 540 nm (IAA production). A scale from 0 to 2 was used to quantify the activity of the target traits among the different isolates. This scale ranged from no change observed compared to the negative control (0), to an average change observed, similar to the positive control (1), or a higher change compared to the positive control (2).

The bacterial strains were molecularly characterized by 16S rRNA gene sequences. They were inoculated in single colonies and grown in solid LB medium at 30 °C for two to three days. The genomic DNA of each strain was obtained using Power Soil Pro kit (QIAGEN) and quantified by spectrophotometer (NanoDrop Technologies, Wilmington, DE, USA). The DNA was used for PCR amplifications of the 16S rRNA gene with the forward primer pA (5'-AGAGTTTGTATCCTGGCTCAG-3') and the reverse primer 1492r (5'-TACCTTGTACGACTT-3'). PCRs were

performed in a final volume of 25  $\mu$ l containing: 1 $\times$  PCR-buffer (10 mM Tris-HCl, 50mM KCl, 1.5 mM MgCl<sub>2</sub>, pH 8.3 at 25 °C), 200  $\mu$ M of dNTPs, 0.1 pmol/ $\mu$ l of forward primers, 0.1 pmol/ $\mu$ l of reverse primer, 0.056 U of fast start Exp-Polymerase and 1  $\mu$ l of DNA. The PCR cycling conditions were a first denaturation at 95 °C for 5 min, 35 cycles at three temperatures, 95 °C for 30 s, 53 °C for 30 s, and 72 °C for 1 min. Additionally, a final extension at 72 °C for 10 min was run and a cooling at 10 °C. The amplification products for all samples were checked on 1 % agarose gel electrophoresis with ethidium bromide - containing buffer. For the PCR amplicon purification, the DNA purification the QIAquick kit was used following the manufacturer's instructions. The 16S rRNA gene amplicons were Sanger sequenced (Macrogen Inc.). The resulting 16S rRNA sequences of the strains were compared to those in GenBank (<http://www.ncbi.nlm.nih.gov/GenBank>) and The Ribosomal Database Project (RDP) (Wang et al., 2007).

### 2.3. Determination of AMF spores in soil and AMF colonization in wild chrysanthemum roots

AMF spores were extracted from 50 ml of rhizosphere soil sampled from wild chrysanthemum plants. The soil was diluted in 2 l of water, mixed and the supernatant (containing spores) poured over a 710  $\mu$ m sieve nested on the top of a 45  $\mu$ m sieve. Then, the material retained on the 45  $\mu$ m sieve was transferred to 50 ml falcon tubes and centrifuged with water at 960  $\times$ g for 3 min. The supernatant was discarded and a solution of 60 % sucrose was added to the pellet and mixed. The solution was centrifuged at 800  $\times$ g for 2 min. The supernatant was transferred to the 45  $\mu$ m sieve, washed with demineralized water to remove the excess sucrose, and transferred to a Petri dish. Viable spores were determined under the dissecting microscope (Leica M205e) by counting those with an intact spore wall and clear internal content and spore abundance was expressed as the number of spores per gram of soil (Gerdemann and Nicolson, 1963). Spores with comparable morphologies were pooled and placed in slides with polyvinyl lacto-glycerol (PVLG) and PVLG with Melzer's reagent (1:1). The mounted spores were observed using a trinocular compound microscope (OPTIKA B-383PLi), and images were captured at different magnifications using an OPTIKA 4083.13E HDMI Easy camera. Identification of spores was performed by comparing their characteristics with published descriptions from the International Culture Collection of Vesicular Arbuscular Mycorrhizal Fungi (INVAM) ([invam.ku.edu](http://invam.ku.edu)).

AMF root colonization was determined by staining the roots using the Ink and Vinegar method (Vierheilig et al., 1998). Small root pieces were cleaned in 10 % KOH for 20 min in a water bath at 90 °C. Cleared root pieces were washed five times with tap water to remove KOH before being submerged in 1 % HCl at room temperature for 5 min to achieve enough acidification for staining. Roots were instantly dyed in 5 % acetic acid after being treated in a blue ink solution at 90 °C for 15 min. To assess root colonization, roots were withdrawn from the acetic acid, placed on glycerol-coated microscopic slides, covered with a cover slip, and examined using an Olympus BH-2 microscope.

To measure mycorrhizal colonization, we used the grid line method (Giovannetti and Mosse, 1980) using a Petri dish with a checkered grid of 1.1  $\times$  1.1 cm at the base. Using this grid size, both the percentage of mycorrhizal colonization and the length of colonized root can be obtained. Pictures were taken by Leica Axiocam MRc5 camera.

### 2.4. AMF propagation in trap cultures

Trap cultures were established according to Stutz and Morton (1996) using Millet (*Panicum miliaceum*) as the host species to propagate AMF. Before sowing, seeds were surface sterilized by immersing in 70 % ethanol for 2 min followed by 2.5 % sodium hypochlorite for 20 min. Seeds were rinsed 5 times with sterile demineralized water and placed in pots containing 1.75 kg of sterile soil and quartzite sand mixture (v/v, 1:9). Each pot received 10-seeds of millet and plants were kept under

greenhouse-controlled temperature, light and humidity conditions (21 °C/16 °C (-1/+2 °C) day/night; 16 h d-1 light, at  $\geq$ 50 % relative humidity). After three months, a subsample of 50 ml was obtained to extract and identify AMF spores as described above, and AMF root colonization was determined by staining the roots using the Ink and Vinegar method (Vierheilig et al., 1998).

Part of the substrate of the first growth cycle was diluted with a sterile soil and quartzite sand mixture (v/v, 1:9) in 1.75 kg pots and reseeded with millet for a second three-month growth cycle of trapping. DNA extraction was performed from a 5 g soil mixture of the propagation using Power Soil Pro kit (QIAGEN) following the manufacturer instructions, to determine the AMF accompanying microbial community composition by analyzing the 16S rRNA partial gene for bacteria, ITS region for fungi, and AMF target phylogenetic marker sequences (see details below).

### 2.5. Chrysanthemum cultivars

Five commercial chrysanthemum (*Chrysanthemum indicum* L.) cultivars, Barolo, Chic-42 (Chic), Chic-045 (Chic 45), Chic Cream and Haydar, were used in this study. Cuttings of each cultivar were planted in 5-cm commercial blocks of peat for 14 days to develop the root system.

### 2.6. Inoculation of bacteria and AMF in chrysanthemum cultivars

After the *in vitro* screening for plant growth traits and phylogenetic analysis, three isolates were selected to be tested in chrysanthemum: Isolates SMF003, SMF006, and SMF018. *Herbaspirillum frisingense* strain IAC/BECa 152 (Schlemper et al., 2018) was used as a positive control while sterile LB medium was used as a negative control.

To produce the bacteria inoculum, all bacterial isolates were collected from individual colonies grown in Petri dishes containing LB medium at 30 °C for two days. The bacterial cells from each strain were cultured overnight at 31 °C in LB liquid medium. Subsequently, they were inoculated into fresh LB medium and allowed to grow until they reached the desired density of the inoculum (10<sup>8</sup> CFUml<sup>-1</sup>). A volume of 2 ml was used for each bacterial strain, and the bacterial inoculants were directly applied onto the roots of the different chrysanthemum cultivar cuttings, on top of the substrate, after placing them 2 cm deep in PVC pots containing 400 g of autoclaved soil and sand mixture (v/v 3:1) (Table S2). A completely randomized design was used with five cultivars, four bacterial strains, and negative control in five replicates.

For the AMF inoculum, soil containing AMF propagules (spores, hyphae, and pieces of colonized roots), was obtained from the trap culture in millet (detailed in Section 2.4). The inoculum was checked microscopically for the presence and number of viable AMF spores following the methods in Section 2.3. A total of 150 ml of AMF soil inoculum was mixed with 400 g of autoclaved soil and sand mixture (v/v 3:1) for each replicate, with an average spore concentration of 3.5 ml<sup>-1</sup> of soil. Cuttings of five cultivars, in five replicates were placed 2 cm deep in PVC pots with the soil mixture containing AMF. For the control treatment, the same volume of AMF inoculum was gamma sterilized and mixed with the autoclaved soil and sand mixture. The plants inoculated with bacterial strains and AMF were grown in a greenhouse (21 °C/16 °C (-1/+2 °C) day/night; 16/8 h light/dark, at 50 % relative humidity) for 22 days.

### 2.7. Plant biomass, soil and plant tissue nutrient analysis

The inoculated plants were harvested after 22 days. For determination of plant biomass, the roots were washed, and the roots and shoots were dried at 60 °C for 48 h for dry biomass measurement. Soil and plant tissue were collected after the harvest and analyzed for macro and micronutrients contents. The soil pH was measured in 0.01 M CaCl<sub>2</sub> (van Raij et al., 2001). Ion exchange resins were utilized to extract the available P-phosphate and exchangeable cations (K<sup>+</sup>, Ca<sup>+</sup>, and Mg<sup>2+</sup>)

(Raj et al., 2009). The P-phosphate content was measured calorimetrically, while the cation concentrations were determined using atomic absorption spectrometry (Shimadzu AA-7000) (van Raji et al., 2001). Soil sulfur-sulfate ( $\text{SO}_4^{2-}$ ) extraction was carried out using a calcium phosphate extraction at 0.01 mol in a 1:2.5 soil/solution ratio and was afterward evaluated using the turbidimetric technique with  $\text{BaSO}_4$  (Bardsley and Lancaster, 1960). The micronutrients Fe, Mn, Cu, and Zn were extracted and measured by atomic absorption spectrometry in a combination of DTPA 0.005 M+ Triethanolamine (TEA) 0.1 M+  $\text{CaCl}_2$  0.01 M. The Shoemaker-McLean-Pratt buffer solution technique (Shoemaker et al., 1961) was used to calculate total acidity at pH 7.0 (H + Al).

The exchangeable  $\text{Al}^{3+}$  was extracted with neutral 1 mol  $\text{l}^{-1}$  KCl at 1:10 soil/solution ratio and determined by titration with a 0.025 mol  $\text{l}^{-1}$  NaOH solution. After extraction of KCl solution, the content of ammonium ( $\text{NH}_4^+$ ) and nitrate ( $\text{NO}_3^-$ ) was also determined by colorimetry by sodium salicylate method and vanadium chloride reduction respectively (Mulvaney, 1996). AMF root colonization was determined by staining the roots using the Ink and Vinegar method (Vierheilig et al., 1998).

## 2.8. Root microbiome assembly of cultivars of *chrysanthemum*

Each plant's rhizosphere was harvested by removing the entire plant from the pot, shaking the plants, and collecting the attached soil with a sterile brush. We considered as bulk soil samples the soil without contact with the roots. Rhizosphere and soil samples were weighed and kept at  $-80^\circ\text{C}$  for later examination.

The rhizosphere total DNA was extracted using the Power Soil Pro kit (QIAGEN) according to the manufacturer's instructions. The quantity and quality of the DNA were assessed using an ND1000 spectrophotometer (NanoDrop Technologies, Wilmington, DE, USA). For the amplification of DNA samples, the following primer sets were employed: 515F (5'-GTGCCAGMCCCGGTAA-3') and 806R (5'-GGAC-TACHVGGGTWTCTAAT-3') targeting the V3-V4 region of the 16S rRNA partial gene for Archaea/bacteria, ITS1F (5'-CTTGGTCATTTA-GAGGAAGT-3') and ITS2 (5'-GCTCGCTTCTTCATCGATGC-3') for the ITS region targeting fungi. To specifically target AMF, a nested PCR approach was utilized. The first PCR employed the universal primer NS31 and the fungus-specific primer AM1 (Helgason et al., 1998), while the second PCR utilized the primers AMV4.5NF and AMDGR (Lumini et al., 2010).

For the amplification of the 16S rRNA gene, PCR was performed as follows: an initial denaturation step at  $94^\circ\text{C}$  for 2 min, followed by 26 cycles of denaturation at  $94^\circ\text{C}$  for 30 s, annealing at  $58^\circ\text{C}$  for 30 s, extension at  $72^\circ\text{C}$  for 30 s, and a final extension step at  $72^\circ\text{C}$  for 7 min. The PCR mixture consisted of 1  $\times$  Roche 10 $\times$  Buffer with 18 mM  $\text{MgCl}_2$ , 5 % Roche DMSO, 0.2 mM dNTP mix from 10 mM NEB, 0.02 U/ $\mu\text{l}$  Roche FastStart High Fi 5 U- $\mu\text{l}$ , 0.6  $\mu\text{M}$  of 515FP primer, 0.6  $\mu\text{M}$  of 806RP primer, and sterile Milli-Q water to reach a final volume of 25  $\mu\text{l}$ .

For ITS amplification, the PCR conditions were an initial denaturation step at  $96^\circ\text{C}$  for 15 min, followed by 33 cycles of denaturation at  $96^\circ\text{C}$  for 30 s, annealing at  $52^\circ\text{C}$  for 30 s, extension at  $72^\circ\text{C}$  for 60 s, and a final extension step at  $72^\circ\text{C}$  for 10 min. The PCR mixture contained 1  $\times$  Qiagen 10 $\times$  Buffer with 15 mM  $\text{MgCl}_2$ , 5 % Roche DMSO, 0.2 mM dNTP mix from 10 mM NEB, 0.02 U/ $\mu\text{l}$  Qiagen HotStar Taq 5 U/ $\mu\text{l}$ , 0.6  $\mu\text{M}$  of ITS1 primer, 0.6  $\mu\text{M}$  of ITS2 primer, and sterile Milli-Q water to reach a final volume of 25  $\mu\text{l}$ . Amplification verification was conducted using a 2 % agarose gel.

For ITS the PCR conditions were an initial denaturation step at  $96^\circ\text{C}$  for 15 min, followed by 33 cycles of  $96^\circ\text{C}$  for 30 s,  $52^\circ\text{C}$  for 30 s,  $72^\circ\text{C}$  for 60 s, and a final extension step at  $72^\circ\text{C}$  for 10 min. The PCR mix contained 1  $\times$  of Qiagen 10 $\times$  Buffer with 15 mM  $\text{MgCl}_2$ , 5 % Roche DMSO, 0.2 mM dNTP mix 10 mM NEB, 0.02 U/ $\mu\text{l}$  Qiagen HotStar Taq 5 U/ $\mu\text{l}$ , 0.6  $\mu\text{M}$  of the ITS1, 0.6  $\mu\text{M}$  of the ITS2 and sterile Milli-Q water up to the final volume of 25  $\mu\text{l}$ . Verification of amplification was performed on 2 % agarose gel.

For the amplification of AMF, the first-round PCR targeted the fungal

small subunit ribosomal DNA (SSU rDNA) fragments. The primers NS31 and AurM1 described by Higo et al. (2019) were used. The first PCR consisted of an initial denaturation step at  $94^\circ\text{C}$  for 5 min, followed by 35 cycles of denaturation at  $94^\circ\text{C}$  for 30 s, annealing at  $60^\circ\text{C}$  for 30 s, extension at  $72^\circ\text{C}$  for 60 s, and a final extension step at  $72^\circ\text{C}$  for 10 min. The PCR mixture included 1  $\times$  Roche 10 $\times$  Buffer with 18 mM  $\text{MgCl}_2$ , BSA (20 mg/ml) at 0.4 mg/ml, 0.2 mM dNTP mix from 10 mM NEB, 0.04 U/ $\mu\text{l}$  of Roche FastStart High Fi 5U- $\mu\text{l}$ , 0.6  $\mu\text{M}$  of AurM1 primer, 0.6  $\mu\text{M}$  of NS31 primer, and sterile Milli-Q water to reach a final volume of 25  $\mu\text{l}$ . The first PCR products were diluted 10-fold and used as templates for the second-round PCR with the primers AMV4.5NF-FwR1 and AMDGR-RvR2. The second-round PCR conditions were the same as the first-round PCR.

A barcoding step with Illumina adapters was added to each sample to facilitate binding of DNA to the flow cell. The PCR was carried out under the following conditions: an initial denaturation step at  $95^\circ\text{C}$  for 10 min, followed by 15 cycles of denaturation at  $95^\circ\text{C}$  for 15 s, annealing at  $60^\circ\text{C}$  for 30 s, extension at  $72^\circ\text{C}$  for 60 s, and a final extension step at  $72^\circ\text{C}$  for 3 min. The PCR mixture consisted of 2  $\mu\text{l}$  of Roche 10 $\times$  Buffer without  $\text{MgCl}_2$ , 1.44  $\mu\text{l}$  of Roche  $\text{MgCl}_2$  (25 mM), 1.00  $\mu\text{l}$  of Roche DMSO, 0.40  $\mu\text{l}$  of dNTP mix from 10 mM NEB, 0.10  $\mu\text{l}$  of Roche FastStart High Fi 5U/ $\mu\text{l}$ , and sterile Milli-Q water to reach a final volume of 20  $\mu\text{l}$ . Verification of barcode incorporation for each sample was conducted on a 2 % agarose gel.

Quantification of each amplicon was performed using the Quant-iT PicoGreen dsDNA Assay Kit (Life Technologies Corporation, Thermo Fisher Scientific, USA). The library was generated by pooling equal quantities (ng) of each amplicon. The pooled library was cleaned up using sparQ PureMag Beads (Quantabio, USA). Library quantification was carried out using the Kapa Illumina GA with Revised Primers-SYBR Fast Universal kit (Kapa Biosystems, UK). The average fragment size was determined using a LabChip GX instrument (PerkinElmer, Inc). Before sequencing, 12 % of PhiX control library was added to the amplicon pools at a final concentration of 9 pM. Sequencing was performed with the MiSeq Reagent kit v3 600 cycles from Illumina (300 bp paired-end) at the Génome Québec Center (Montreal, Quebec).

## 2.9. Bioinformatics and data integration analysis

Differences between the shoot and root biomass of the five cultivars were analyzed using the ExpDes.pt v1.2.2 package using the function fat2.crd (Ferreira et al., 2014) in R v3.6.1 (Team, 2019). The normality of the data was checked with Shapiro-Wilk test with 5 % significance. The pairwise testing was done using Tukey-test with  $P \leq 0.05$  considered significant and plotted using ggplot2 v3.2.1 package (Wickham, 2009).

The quality assessment of reads was conducted using the FASTQC quality control tool version 0.10.0 (Babraham Bioinformatics - FastQC a Quality Control Tool for High Throughput Sequence Data [WWW Document], n.d.) for 16S rRNA, ITS, and AMF amplicon sequences. Subsequently, Cutadapt (Martin, 2011) was employed to truncate the forward and reverse reads. The DADA2 v1.16.0 pipeline (Callahan et al., 2016) was utilized for denoising and obtaining amplicon sequence variants (ASVs) from demultiplexed reads across all samples. Reads lacking overlap were excluded from further analysis. Taxonomic classification was performed using the naïve Bayesian classifier implemented in DADA2, utilizing the 'Silva version 138' database for Archaea/bacteria (Quast et al., 2013), the UNITE v8.2 database for fungi (Nilsson et al., 2019), and MAARJAM for AMF (Öpik et al., 2010). The ASV table was filtered at the Genus level and used for subsequent analysis. To merge low-occurring microbes that couldn't be properly modeled, a threshold of 10 occurrences was applied using the decostand function from the Vegan package (Oksanen et al., 2012), resulting in a column named 'Others'. Microbiome analyses were carried out in R v.4.2.0 (Team, 2019). Data analyses and graphical displays were done using the following R packages: tidy, dplyr, and ggplot2 (Wickham, 2009).

For estimating the effects of plant cultivar and inoculum in different

treatments (bacterial isolates and AMF), the gjam package v2.3.2 (Clark et al., 2017) was employed. GJAM consists of a Generalized Joint Attribute Modelling that allows to integration data from different types (e.g., continuous, binary, ordinal, compositional). In our case, we integrated as response variables the continuous values of biomass variables which included root dry weight (g), shoot dry weight (g); plant nutrients such as Nitrogen (N), Phosphorus (P), Potassium (K), Calcium (Ca), Magnesium (Mg), Sulfur (S), Iron (Fe), Manganese (Mn), Copper (Cu), Zinc (Zn), Boron (B), Aluminum (Al), and Sodium (Na); and soil nutrients that encompassed Total Nitrogen (N tot), Phosphorus (P), Potassium (K), Calcium (Ca), Magnesium (Mg), Sulfur (S), Aluminum (Al), Sodium (Na), Copper (Cu), Zinc (Zn), Boron (B), Iron (Fe), Manganese (Mn), Molybdenum (Mo), Cadmium (Cd), Chromium (Cr), Nickel (Ni), and Lead (Pb) with the microbiome data which is compositional (Gloor et al., 2017). Two different models were created (one for bacterial inoculation and the other for the AMF inoculation) returned the regression coefficients corresponding to the shifts in the microbial community, plant biomass, and plant and soil nutrients as a result of the

different treatment combinations (factorial design). The major advantage of the GJAM model is the possibility to analyse the response variable on the scale it is measured. For example, the regression coefficients for the root dry weight represent the increase or decrease in grams as a result of the inoculation with bacterial isolates or AMF. Similarly, the regression coefficients for the microbial communities represent the increase or decrease in relative abundance (percentage of change in the original abundance). Therefore, for the microbiome, positive coefficients were depicted to represent significantly different microbial groups selected in the rhizosphere of each treatment, while negative coefficients represented significantly different microbial groups not selected in the rhizosphere of each treatment. Model diagnosis involved evaluating the Markov Chain Monte Carlo (MCMC) to determine the stability of estimated coefficients after 15,000 interactions (with a burn-in of 6000 interactions). As the experiment followed a two-way factorial design, regression coefficients were compared against the null hypothesis H0, which assumed no difference between inoculum and control within each plant genotype. Significance of the regression coefficients

**Table 1**

List of bacterial isolates, species similarity and identity percentage retrieved from NCBI, origin of the isolate, and plant growth-promoting activity score. The selected strains tested in this study are indicated in bold. A quantitative scale was used to measure the activity of the traits, ranging from 0 (no change compared to negative control) to 2 (a higher change compared to positive control).

| Isolate      | Strain   | Identity (%) | Compartment      | Siderophore | Indol Acetic Acid | P solubilization |
|--------------|--|--------------|------------------|-------------|-------------------|------------------|
| SMF001       | <i>Neobacillus niacini</i> strain FO118                          | 97           | Endosphere       | 1           | 0                 | 0                |
| SMF002       | <i>Bacillus cereus</i> strain YT514                              | 90           | Endosphere       | 0           | 0                 | 0                |
| SMF003       | <b><i>Priestia megaterium</i> strain 3</b>                       | 96           | Endosphere       | 1           | 1                 | 1                |
| SMF004       | <i>Bacillus toyonensis</i> strain FJAT-29993                     | 98           | Endosphere       | 0           | 0                 | 0                |
| SMF005       | <i>Paenibacillus</i> sp. NA11019                                 | 91           | Endosphere       | 1           | 0                 | 0                |
| SMF006       | <b><i>Priestia megaterium</i> strain EG1278</b>                  | 98           | Endosphere       | 1           | 1                 | 1                |
| SMF007       | <i>Rhizobium herbae</i> strain FC18                              | 93           | Endosphere       | 1           | 0                 | 0                |
| SMF008       | <i>Xanthomonas axonopodis</i> strain BLKC3                       | 97           | Endosphere       | 0           | 1                 | 0                |
| SMF009       | <i>Xanthomonas axonopodis</i> strain DHKQ4                       | 90           | Endosphere       | 0           | 1                 | 0                |
| SMF010       | <i>Gordonia aichiensis</i> strain 344BRRJ                        | 92           | Endosphere       | 1           | 0                 | 1                |
| SMF011       | <i>Xanthomonas citri</i> pv. <i>punicae</i> strain Xap7          | 91           | Endosphere       | 0           | 0                 | 0                |
| SMF012       | <i>Pseudarthrobacter equi</i> strain IMMIB L-1606                | 91           | Endosphere       | 1           | 1                 | 1                |
| SMF013       | <i>Xanthomonas oryzae</i> pv. <i>oryzicola</i> strain JX-2016-94 | 95           | Endosphere       | 0           | 0                 | 0                |
| SMF014       | <i>Pseudomonas reinekei</i> strain MT1                           | 94           | Rhizosphere      | 0           | 1                 | 1                |
| SMF015       | <i>Pseudomonas lurida</i> strain A10                             | 97           | Rhizosphere      | 2           | 0                 | 2                |
| SMF016       | <i>Pseudomonas capeferrum</i> strain N30                         | 95           | Rhizosphere      | 1           | 0                 | 1                |
| SMF017       | <i>Pseudomonas syringae</i> strain S13                           | 96           | Rhizosphere      | 2           | 0                 | 1                |
| SMF018       | <b><i>Pseudomonas</i> sp. RBE1CD-131</b>                         | 95           | Rhizosphere      | 2           | 2                 | 2                |
| SMF019       | <i>Microbacterium foliorum</i> strain CH6                        | 98           | Rhizosphere      | 1           | 0                 | 0                |
| SMF020       | <i>Rahnella inusitata</i> strain VT25B                           | 98           | Rhizosphere      | 1           | 1                 | 1                |
| SMF021       | <i>Erwinia aphidicola</i> strain TO2                             | 97           | Rhizosphere      | 0           | 0                 | 2                |
| SMF022       | <i>Paenarthrobacter nitroguajacolicus</i> strain SR21            | 84           | Rhizosphere      | 1           | 1                 | 1                |
| SMF023       | <i>Bacillus</i> sp. strain isolate 158                           | 97           | Rhizosphere      | 1           | 1                 | 1                |
| SMF024       | <i>Arthrobacter halodurans</i> strain CEMTC_6971                 | 98           | Rhizosphere      | 1           | 0                 | 0                |
| SMF025       | <i>Pseudomonas fluorescens</i> strain LBUM647                    | 98           | Rhizosphere      | 1           | 0                 | 0                |
| SMF026       | <i>Pseudomonas putida</i> NGB-MS2                                | 86           | Rhizosphere      | 2           | 0                 | 2                |
| SMF027       | <i>Pseudomonas frederiksbergensis</i> strain CEMTC_4625          | 98           | Soil             | 1           | 1                 | 2                |
| SMF028       | <i>Psychrobacillus psychrodurans</i> strain Rz1.1-3              | 92           | Soil             | 1           | 1                 | 0                |
| SMF029       | <i>Lelliottia amnigena</i> strain FB1                            | 86           | Soil             | 1           | 0                 | 1                |
| SMF030       | <i>Pseudomonas</i> sp. strain A2                                 | 99           | Soil             | 1           | 1                 | 1                |
| SMF031       | <i>Bacillus</i> sp. MNPK-12                                      | 94           | Soil             | 1           | 1                 | 1                |
| IAC/BECa 152 | <i>Herbaspirillum frisingense</i>                                |              | Positive control | 1           | 1                 | 1                |

was determined when the 95 % confidence interval did not include zero.

The GJAM regression coefficients reflected the impact of different treatments on shaping the microbiome (Rotoni et al., 2022), the soil nutrients, and the plant features (biomass and nutrient concentration). A Principal component analysis (PCA) was used to explore community similarities between cultivars and treatments while visualizing the variance among the set of regression coefficients representing microbiome profiles and shifts in plant biomass and nutrients. Besides, to look for the different microbial taxa that responded to the treatments we also used bubble plots to relate the shift in their relative abundance with their original relative abundance in the control treatment. To visualize the shifts in community abundance within each treatment, centered log-ratio (CLR) transformation was employed.

### 3. Results

#### 3.1. Bacterial strains PGP traits and molecular characterization

A total of 31 bacterial strains were isolated from wild chrysanthemum in different compartments: 13 from the rhizosphere, 13 from the endosphere, and five from the soil. Molecular characterization of these 31 bacterial strains based on 16S rRNA gene sequences showed that the most common bacterial genera were *Bacillus* in the endosphere, and *Xanthomonas* and *Pseudomonas* in rhizosphere and soil. Out of the 31 isolates, 23 were capable of producing siderophores, 18 solubilize phosphate and 14 produce IAA (Table 1).

A total of 10 isolates exhibited activity for all three PGP traits tested

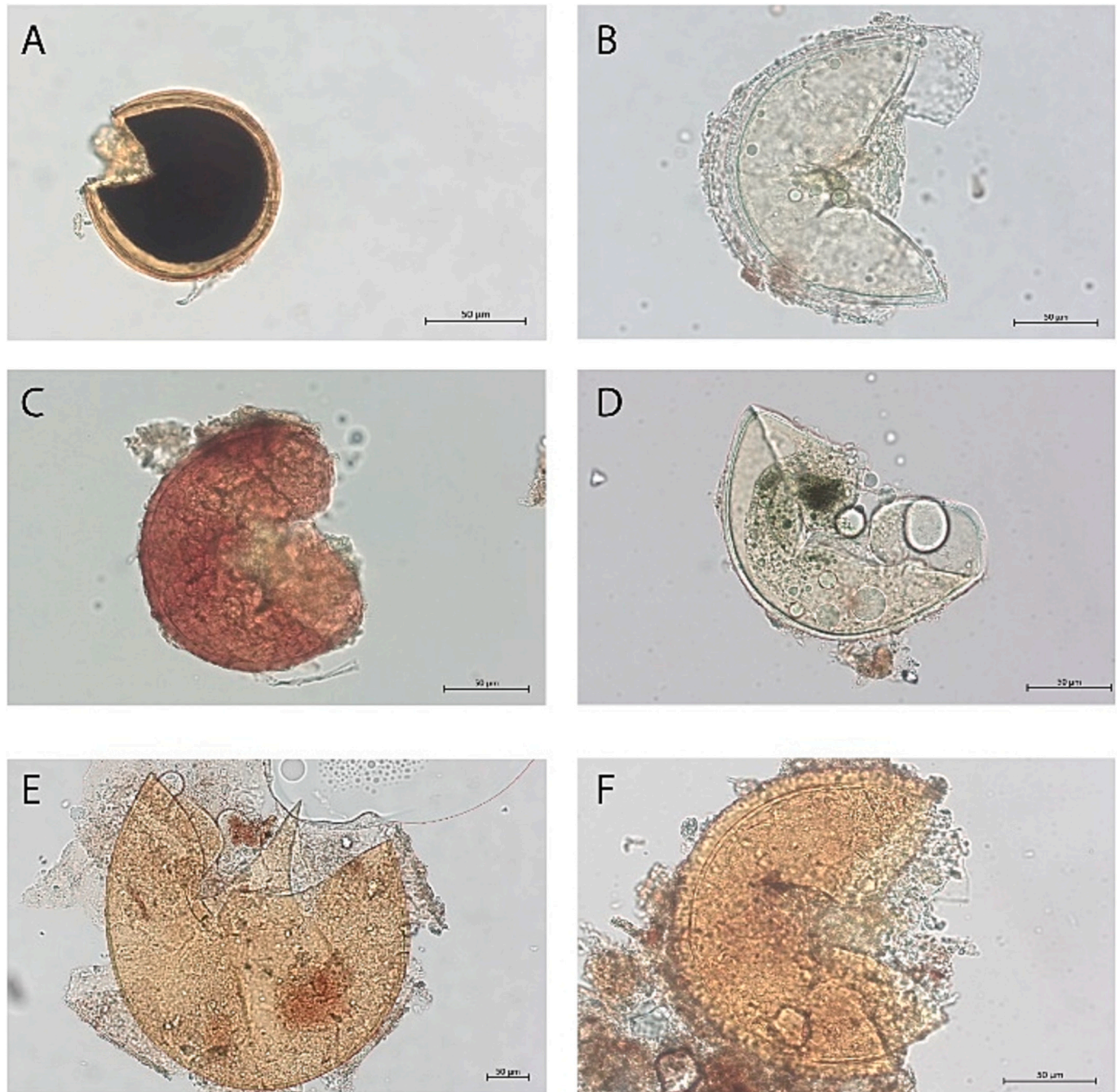


**Fig. 1.** Spores of arbuscular mycorrhizal fungal species identified in soil from trap cultures. (A) *Acaulospora morrowiae*, (B) *Glomus* sp1, (C) *Claroideoglomus etunicatum*, (D) *Rhizophagus clarus*, (E) *Funneliformis* sp1, and (F) *Glomus* sp2.

(Fig. S1, Table 1). Strains SMF003 and SMF006 showed 95 % and 98 % of similarity with *Priestia megaterium* strain 3 and *Priestia megaterium* strain EGI278, respectively. Strain SMF018 was similar (97 %) to *Pseudomonas* sp. RBE1CD-131. These three isolates were selected for further plant growth experiment.

### 3.2. AMF spore characterization, root colonization, and AMF accompany microbiome (AMFc)

A total of six spore morphotypes belonging to five genera (Fig. 1) were recovered from rhizosphere soil of wild chrysanthemum and propagated in trap cultures. Spores were identified as *Acaulospora morrowiae*, *Claroideoglossum etunicatum*, *Rhizophagus clarus*, *Funelliformis* sp. (resembling *F. mosseae*), *Glomus* sp1 and *Glomus* sp2. The spore morphotypes were found in trap cultures associated with millet roots, with an average number of 3.50 spores ml<sup>-1</sup> of soil.

To verify AMF root colonization, we used the “Ink and Vinegar” staining method on the roots of wild chrysanthemum and millet (host for propagation). Microscopic observations revealed the presence of intraradical and extraradical hyphae, arbuscules at different morphological stages of formation, and vesicles in the roots of wild chrysanthemum and millet. The overall colonization of roots from wild chrysanthemum was 75 % (Fig. 2A, B). Stained roots from millet showed approximately 60 % colonization, with intraradical hyphae and vesicles present (Fig. 2C, D).

The AMFc was used as inoculum during multiplication with millet. Before the use of this inoculum, we characterized the composition of the bacterial and fungal communities associated with AMF. The bacterial AMFc accompany community was mainly from phyla Actinobacteria, Chloroflexi, Proteobacteria, and Firmicutes, while the fungal community was from phyla Ascomycota, Basidiomycota, and Mortierellomycota. The main two AMF genera found in the community, based on SSU rRNA amplicon sequences, were an unidentified genus of the Glomeromycetes class and *Paraglomus* as shown in Fig. S2.

### 3.3. Effect of bacterial isolates SMF003, SMF006 and SMF018, and AMFc on biomass of different chrysanthemum cultivars

The effect of bacterial isolates SMF003, SMF006, and SMF018, the positive control *H. frisingense* strain IAC/BECa 152, and AMFc on shoot and root dry biomass of five different chrysanthemum cultivars varied from positive to negative effects depending on the cultivar. While no significant differences in shoot biomass were observed among the cultivars when inoculated with any of the strains (data not showed), the response of root biomass varied depending on the cultivar and type of inoculation (Fig. 3A).

For instance, the cultivar Chic exhibited a significant decrease in root dry weight when inoculated with SMF018 ( $3.32 \pm 0.92$  g,  $n = 5$ ), *H. frisingense* ( $2.93 \pm 0.56$  g,  $n = 5$ ), and SMF006 ( $2.52 \pm 0.58$  g,  $n = 5$ ), compared to the control ( $4.91 \pm 1.61$  g,  $n = 5$ ). On the other hand, Chic Cream inoculated with SMF006 ( $3.84 \pm 1.39$  g,  $n = 5$ ) showed a 57 % increase in root dry weight compared to the control ( $2.45 \pm 0.55$  g,  $n = 5$ ). Similarly, Haydar cultivar inoculated with SMF006 ( $4.1 \pm 0.48$  g,  $n = 5$ ) and SMF018 ( $4.12 \pm 0.99$  g,  $n = 5$ ) had an increase of 62 % and 63 %, respectively, in root dry weight compared to the control ( $2.54 \pm 0.58$  g,  $n = 5$ ). However, the cultivars Barolo and Chic 45 did not show significant differences in root biomass between bacterial inoculation and controls.

The impact of AMFc inoculation on root biomass was assessed in five different cultivars of chrysanthemum (Fig. 3B). Cultivar-dependent responses were observed, with Chic 45 and Chic Cream showing a significant increase in root biomass. Chic 45 exhibited a 40 % increase in root biomass ( $2.9 \pm 0.51$  g,  $n = 5$ ) compared to the control ( $2.07 \pm 0.2$  g,  $n = 5$ ), while Chic Cream showed a significant increase of 79 % ( $4.46 \pm 0.9$  g,  $n = 5$ ) compared to control ( $2.5 \pm 0.38$  g,  $n = 5$ ). However, no significant differences in root biomass were observed between Barolo, Chic, and Haydar cultivars when inoculated with AMFc compared to controls. Interestingly, Chic Cream exhibited a significant increase in root biomass following both SMF006 and AMFc inoculations. The

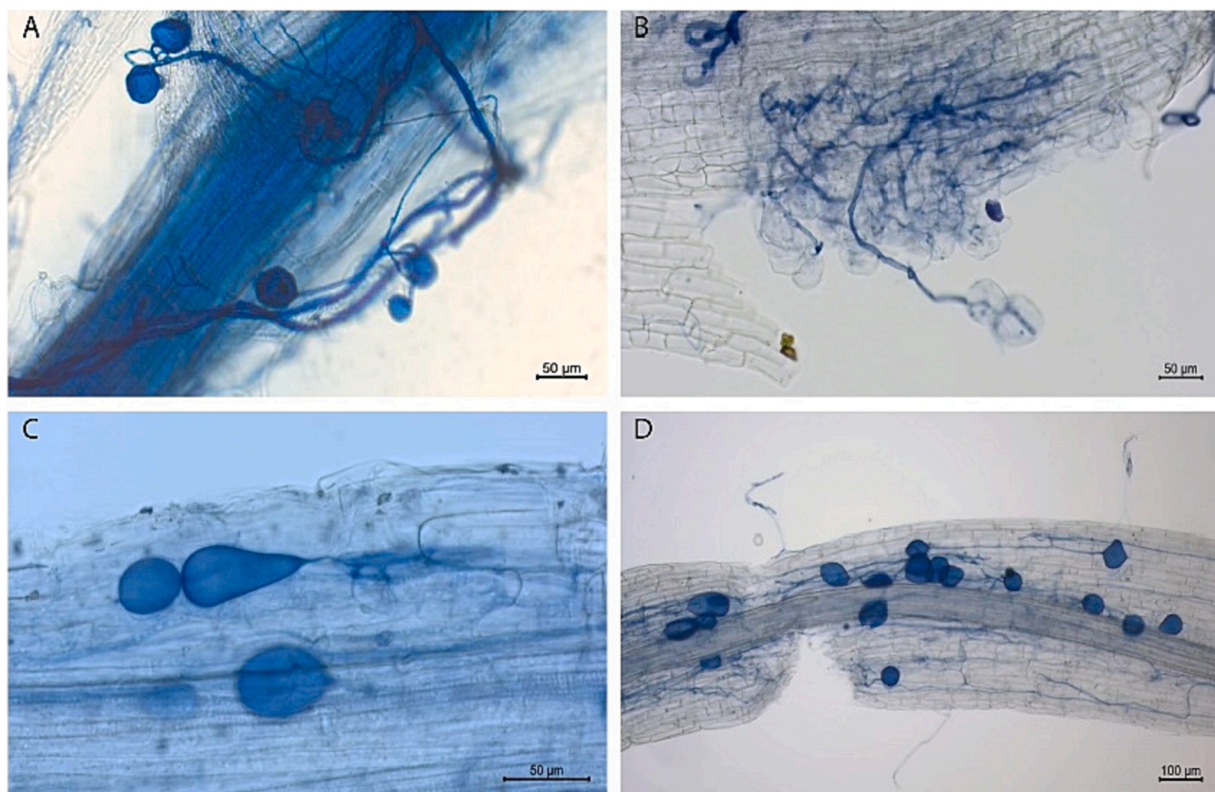
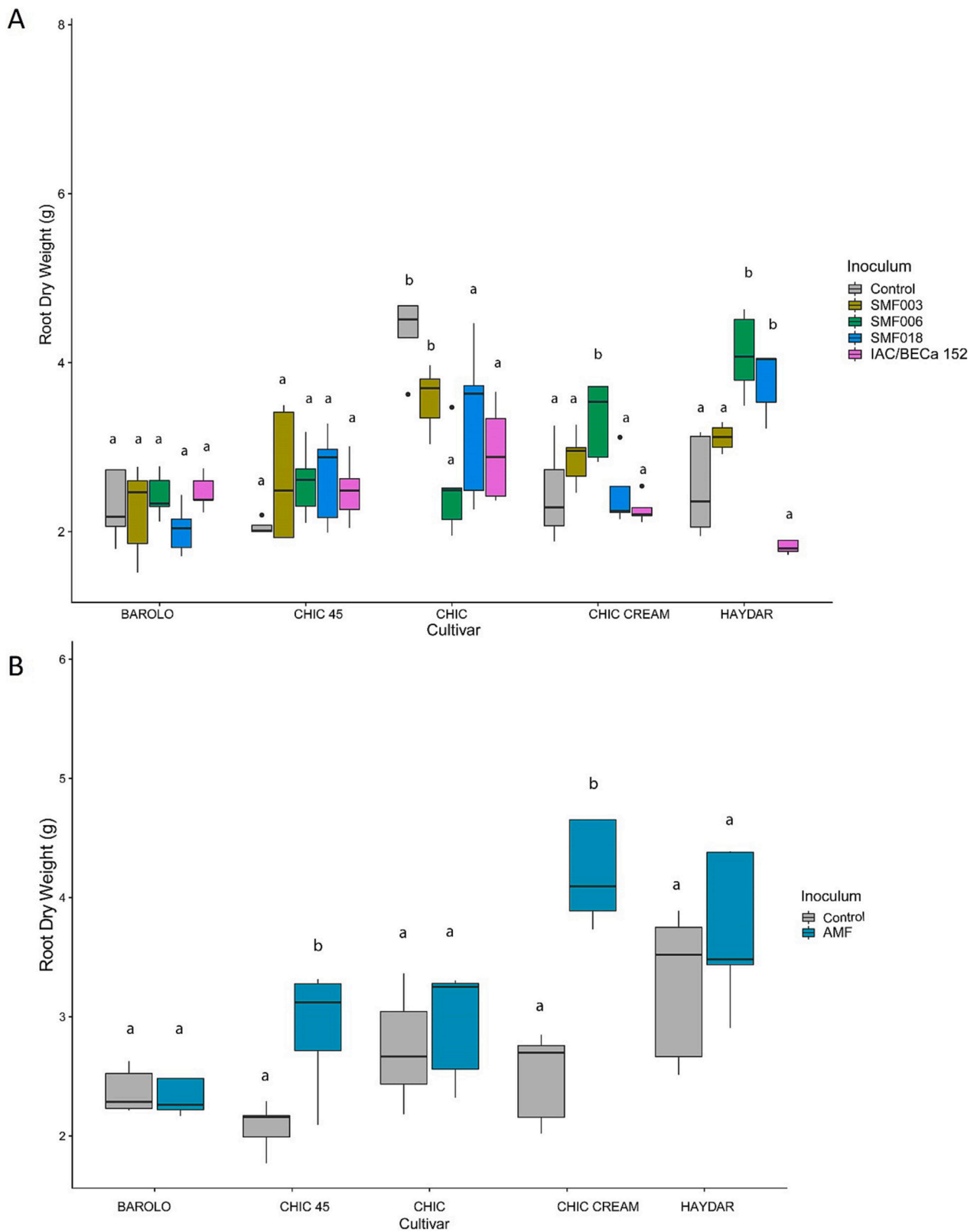


Fig. 2. Arbuscular mycorrhizal fungal structures (A, B, C, D) in stained roots from trap cultures in millet.



**Fig. 3.** Root dry biomass (g) per chrysanthemum cultivars after inoculation with (A) bacterial isolates SMF003, SMF006, SMF018 and IAC/BEca 152 (*Herbaspirillum frisingense* strain IAC/BEca 152 as positive control), and (B) AMF. Each color represents a different inoculum. Significant differences between inoculum and control within the same cultivar (Tukey-test,  $p < 0.05$ ) are denoted by different letters.



overall colonization of roots from commercial chrysanthemum was <10 %. No AMF colonization structures were found in the commercial chrysanthemum cultivars, except for early-stage hyphal formation in the cultivars Chic Cream and Haydar.

### 3.4. Rhizosphere microbiome assembly of cultivars of chrysanthemum after inoculation with bacterial strains and AMFc

Principal Component Analysis (PCA) summarized the relative importance of cultivar and inoculation in changing both bacterial and fungal rhizosphere community profiles following bacterial (Fig. 4A–B) and AMFc (Fig. 4C–D) inoculations. In each plot, each dot represented the microbial profile of a single treatment. When plants were inoculated with single isolates, the majority of shifts in the microbial community resembled the differences between the cultivars, with a smaller spread evident due to the inoculation. In short, all bacteria inocula significantly changed the microbial composition of both bacterial and fungal communities in all cultivars. Specifically, the first two axes captured 52 % and 51 % of the total variability of the bacterial and fungal communities, respectively. Notably, the treatments with significant increase in the root biomass presented distinct communities. This spreading in the rhizosphere community likely resulted from cultivar-specific selection being stronger than the impact of the bacterial inoculation.

On the other hand, when we inoculated the complex community of

AMFc (AMF + bacterial and fungal communities), the microbiome profiles of different cultivars showed a more pronounced deviation between treatment and control groups. The cultivar selection resulted in a smaller distinction between them, mainly restricted to the second dimension of the PCA that accounted for 15.5 % and 23.1 % of the total variability for bacterial and fungal communities, respectively. Notably, after AMFc inoculation, the microbial profile of Chic Cream and Barolo cultivars had a distinct profile compared to the other cultivars. These findings suggest that AMFc inoculation significantly influences the assembly of the microbiome in chrysanthemum, leading to the development of unique microbial profiles in specific cultivars.

To trace the presence of AMF in the chrysanthemum rhizosphere after AMFc inoculation, the AMF specific phylogenetic marker was sequenced. Despite root colonization of AMF in commercial chrysanthemum roots being <10 % for cultivars Chic 45, Chic Cream, and Haydar, we detected the presence of the genus *Paraglomus* in the rhizosphere of all five cultivars 22 days after inoculation based on sequencing data (Fig. S3).

### 3.5. Shifts in microbiome profile, plant biomass, and plant and soil nutrients

Using a model-based approach, we distinguished the cultivar-specific rhizosphere microbial profiles of each chrysanthemum cultivar

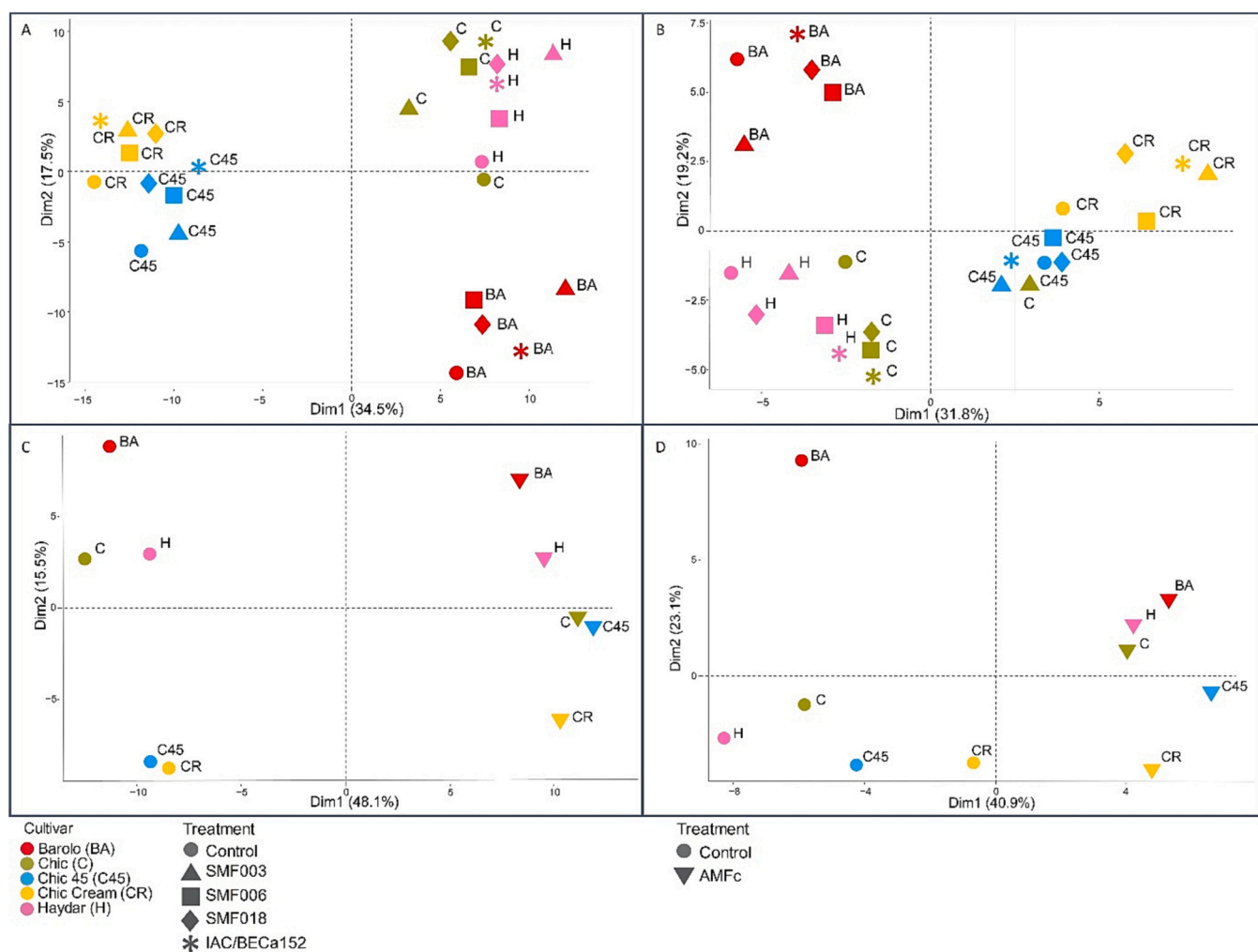


**Fig. 4.** PCA showing differences in (A) bacterial and (B) fungal community assemblies after inoculation with bacterial strains (SMF003, SMF006, SMF018, and IAC/BECa152), as well as differences in the (C) bacterial and (D) fungal community assemblies after inoculation with AMFc and their respective controls. Each shape represents the microbial profile of four replicates of each treatment. Cultivars are indicated by different colors and the abbreviations BA (Barolo), C (Chic), C45 (Chic 45) and CR (Chic Cream), and H (Haydar). IAC/BECa 152: *Herbaspirillum frisingense* strain IAC/BECa 152 as positive control.

following bacterial inoculation. Our results indicate that microbial selection in the rhizosphere was dependent on the cultivar, as shown in Figs. 5 and 6, which represent all the statistically significant shifts in bacterial and fungal genera and their relationship with plant and soil variables, as determined by regression coefficients. To visualize the shifts in community abundance within each treatment, centered log-ratio (CLR) transformation was employed. This transformation was used to show the different microbial taxa that responded to the treatments by comparing the shift in their relative abundance with their original relative abundance in the control treatment.

When we examined the treatments that significantly increased the root biomass of the chrysanthemum cultivars (CR + SMF006, and H + SMF006 or H + SMF018), we observed that the major shifts in the microbial community affected the microbes that were within 2.5 log-fold of the average abundance in the controls. For those three treatments, a total of 84 bacteria and 25 fungi (at the genus level) increased their abundances, followed by the decrease of 60 bacteria and 19 fungi groups (at the genus level). For the fungal community, those treatments also showed some similarities. Interestingly, for the cultivar Chic, we observed shifts in a wider range of microbes, ranging from the highly abundant (>5 log-fold difference from the average) to the low abundant (<2.5 log-fold) bacteria. Table S3 summarizes the main bacterial and fungal families, plant and soil variables, and their changes in abundance compared to the control after bacterial inoculation. In the rhizosphere, the inoculated strains increased the abundance of their corresponding genera. The dominant fungal phyla were Ascomycota, Basidiomycota, and Mucoromycota.

Our analysis of plant biomass not only supported the statistical analysis of root and shoot dry weight but also allowed us to detect changes in the plant nutrient content. Specifically, Chic Cream exhibited increased root biomass when inoculated with SMF006, while Haydar displayed increased biomass with SMF003, SMF006, and SMF018 inoculations. The impact of bacterial inoculations on plant nutrient content was also dependent on cultivar. For instance, SMF006 inoculation increased Cu content in Chic Cream (Fig. S4), while in soil, Ni content increased and Mg content decreased for the cultivar Haydar (Fig. S5).

The effects of AMFc inoculation showed an increased abundance of several bacterial families, namely *Frankiaceae*, *Gemmatimonadaceae*, *Burkholderiaceae*, *Microbacteriaceae*, *Xanthomonadaceae*, and fungal families including *Ceratobasidiaceae*, *Herpotrichiellaceae*, and *Trimorphomycetaceae* (Table S4). Interestingly, both AMFc and bacterial isolates treatments led to a shift in the abundance of genera from the phylum Proteobacteria, with a higher number of genera represented. Furthermore, specific cultivars showed varying responses to AMFc inoculation. For instance, Chic Cream exhibited an increase in root dry weight, as well as an increase in Cu in the plant and a concentration of P and Mn in the rhizosphere soil. Similarly, cultivar Chic 45 demonstrated an increase in root dry weight, as well as increases in Zn, Mg, and Mn in the plant (Fig. S5). These results suggest that AMFc inoculation can have a cultivar-specific impact on plant growth and nutrient uptake.

In summary, our analysis of five different chrysanthemum cultivars revealed that the effects of PGPM inoculation can range from positive to negative and are dependent on the cultivar. Furthermore, the changes in the rhizosphere bacterial and fungal community profiles of chrysanthemum were smaller when inoculated with a single bacterial isolate than when inoculated with a complex community (AMF + Accompany microbiome: AMFc).

#### 4. Discussion

Inconsistency in obtaining reliable results from PGPM inoculation led us to investigate three novel principles: (i) collecting microbes (bacteria and AMF) from a wild relative of our target plant (chrysanthemum) and assessing their potential plant-growth promotion traits; (ii) inoculating the PGPM in a complex environment (living soil substrate); and (iii) evaluating the cultivar preferences to inoculation of

growth promoting microbes of single isolates and a complex community of AMF and accompanying microbes. We found that the plant response is mainly cultivar specific, but it becomes more responsive to PGPM when the inoculum is an already complex community of beneficial microbes.

We searched for bacteria strains and AMFc with plant growth-promoting traits using a wild relative of chrysanthemum growing in an open field in the Netherlands. By focusing on the unexplored functional potential of microbiota from wild plant species (Bonfante, 2018; Chang et al., 2022; Ma et al., 2017), we aimed to restore beneficial associations that may have been lost during the domestication of plants, including plant breeding, the use of pesticides, and fertilizers. From a range of 31 isolated and biochemical and phylogenetically characterized strains, we selected three isolates based on their plant growth-promoting traits, namely SMF003 and SMF006, which were similar to *Priestia megaterium* strain ATCC 14481 and *Priestia megaterium* strain H108, respectively, and SMF018, which was similar to *Pseudomonas* sp. RA12 based on 16S rRNA gene sequences. The application of *P. megaterium* as a plant growth-promoting bacterium has been reviewed recently (Biedendieck et al., 2021) and tested in various crops (Ortiz-Castro et al., 2008; Wang et al., 2021; Zhou et al., 2017), confirming its beneficial impact on plants involving phosphate solubilization, IAA and siderophore production. Despite being commonly known as a pathogen of chrysanthemum (Elsisi, 2019), recent studies have highlighted the potential benefits of *Pseudomonas* in certain contexts (Passera et al., 2019). Moreover, it is possible that the pathogenic species is different from the one we isolated, which showed promotion of chrysanthemum growth. Regardless, this study represents the first attempt to evaluate the application of these specific isolates in commercial chrysanthemum cultivars.

We tested a total of 20 combinations of our four inoculated bacteria (three from the wild chrysanthemum and one positive control) with five chrysanthemum cultivars. However, only three treatments resulted in a positive effect on root growth. Cultivar Chic Cream inoculated with SMF006 exhibited 57 % increase in root biomass, and the Haydar cultivar inoculated with SMF006 and with SMF018 had an increase of 62 % and 63% in root biomass, respectively, compared to the control. However, the same bacteria strains in the cultivar Chic decreased root biomass. Therefore, the effects of these strains may range from positive to negative. Chrysanthemum cultivars used in the flower sector are intensely bred to express commercially relevant traits and phenotypes, which may inadvertently compromise the plant's ability to recruit and respond to beneficial microbes. In our recent study, we showed that different plant breeding techniques resulted in distinct microbial community assembly (Rotoni et al., 2022), moderated by the soil fertility and organic content. Consequently, reinstating microbes from wild relatives should be coupled with the identification of the plant genetic loci that recruit those beneficial microbes. Otherwise, their role as growth promoters will remain cultivar-specific.

We propose to directly test influence of PGPM inoculation in a complex environment, evaluating its impact not only on the growth of different plant cultivars but also on the soil microbiome because the impact of inoculation is cultivar-dependent. The PCA analysis summarized changes in microbiome profiles and revealed that the differences between control and inoculated treatments were smaller than overall differences between cultivars. These results suggest that inoculating single bacterial strain has only a small impact on the microbiome of chrysanthemum plants. Interestingly, SMF006 and SMF018 strains increased the abundance of their respective genera, suggesting that these strains may have the capacity to persist in the soil after inoculation.

Our integrated data model revealed cultivar-dependent changes in plant and soil nutrient levels after bacterial and AMFc inoculations. Notably, we observed an increase in Cu levels in Chic Cream plant tissue after SMF006 and AMFc inoculation, which is of particular interest. Previous studies have reported that inoculating maize with bacteria that can solubilize phosphorus, biosynthesize indole-3-acetic acid, and

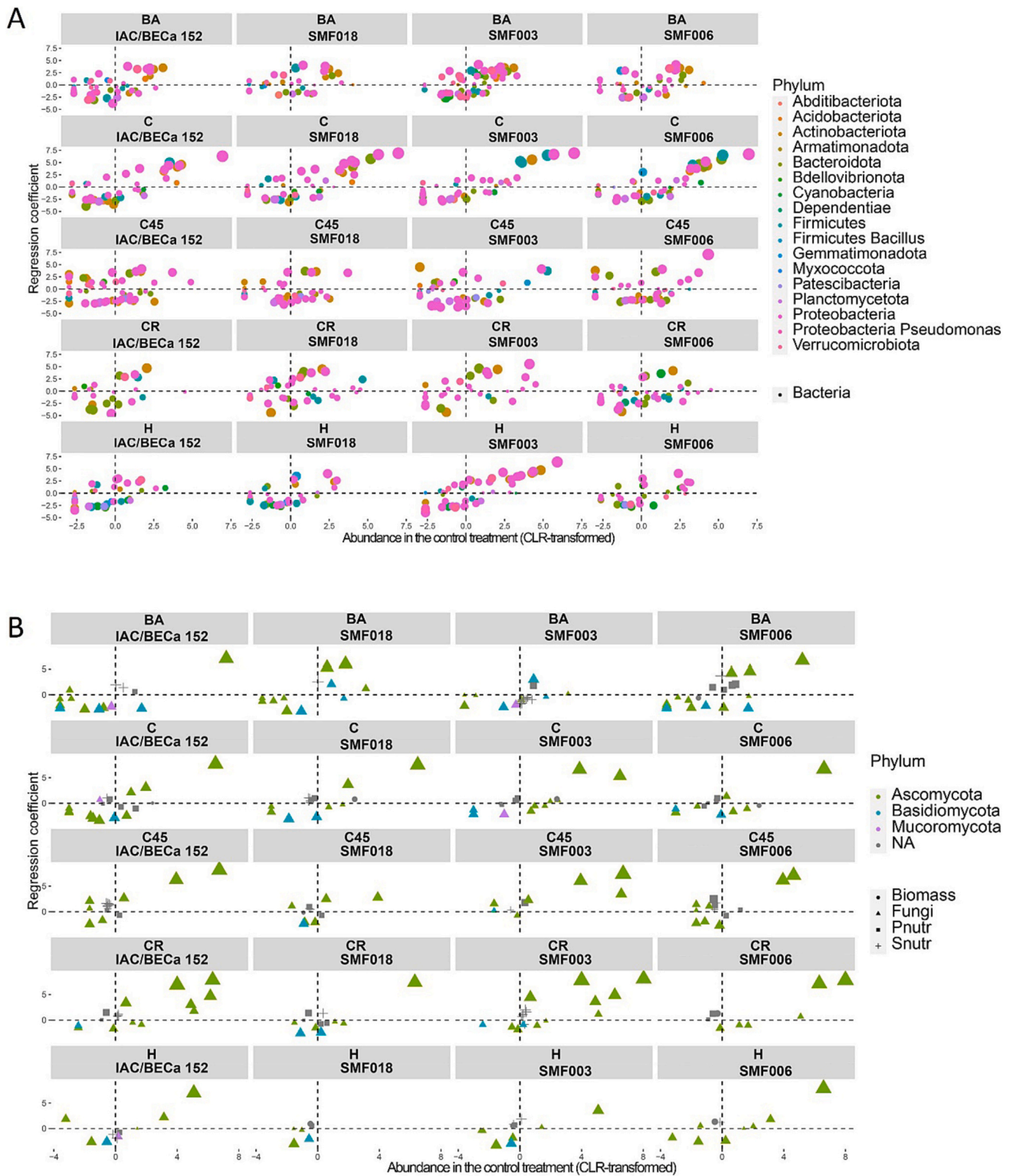


**Fig. 5.** Bubble plots depict shifts in regression coefficients of amplicon sequence variants (ASVs) found in the bacterial treatments (SMF003, SMF006, SMF018, and IAC/BECa152) across five different chrysanthemum cultivars. Different microbial taxa, plant biomass, and plant and soil nutrients that responded to the treatments are represented by shifts in their relative abundance compared to the original relative abundance in the control treatment. Colors represent different (A) bacterial and (B) fungal phyla, while shapes represent plant biomass (Biomass), plant nutrients (Pnutr), and soil nutrients (Snutr). The size of the dots is proportional to the value of the regression coefficient. Cultivars are indicated by the abbreviations BA (Barolo), C (Chic), C45 (Chic 45) and CR (Chic Cream), and H (Haydar). IAC/BECa 152: *Herbaspirillum frisingense* strain IAC/BECa 152 as positive control.

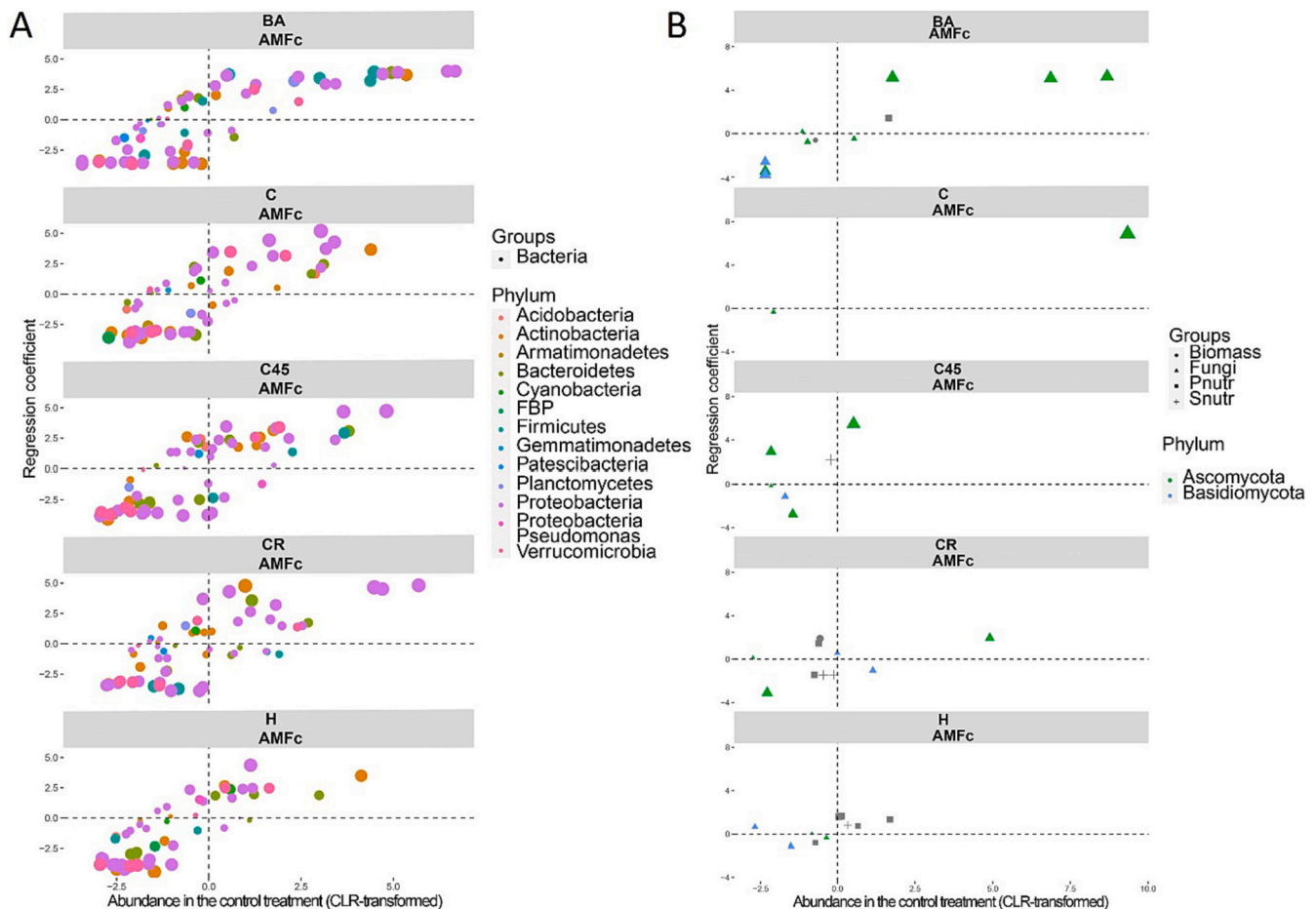


**Fig. 6.** Bubble plots representing shifts in regression coefficients of amplicon sequence variants (ASVs) found in the AMF treatment across five different chrysanthemum cultivars. Different microbial taxa, plant biomass and plant and soil nutrients that responded to the treatments compared to their relative abundance in the control treatment. Colors represent different (A) bacterial and (B) fungal phyla, while shapes represent plant biomass (Biomass), plant nutrients (Pnutr), and soil nutrients (Snutr). The size of the dots is proportional to the value of the regression coefficient. Cultivars are indicated by the abbreviations BA (Barolo), C (Chic), C45 (Chic 45) and CR (Chic Cream), and H (Haydar). H: *Herbaspirillum frisingense* strain IAC/BECa 152 as positive control.

produce siderophores can significantly increase Cu compared to single inoculation (Rojas-Tapias et al., 2014). Furthermore, siderophores such as Ferrichrome, which is a prototype of hydroxamate siderophores, have been shown to chelate Cu, chromium (Cr), aluminum (Al), and gallium (Ga) in addition to Fe (Albelda Berenguer et al., 2019). Interestingly, the SMF006 isolate is similar to *P. megaterium*, which has been shown to produce this class of siderophores (Nascimento et al., 2020).

In our inoculation with AMF we did not consider AMF as an isolated inoculum, but rather as the inoculation of AMF species along with its associated microbiome (bacteria and fungi). The methods we used to propagate and extract the AMF maintained a community of accompanying microbes. The accompany AMF community was mainly composed of bacteria from the phyla of Actinobacteria, Chloroflexi, Proteobacteria, and Firmicutes. Interestingly, the Actinobacteria phylum was one of the most abundant in our AMF inoculum. This group of bacteria is commonly found in association with AMF spores and capable of hydrolyzing chitin, which is the primary constituent of spore walls, and was credited with the improvement of spore germination (Roesti et al., 2005).

We observed the presence of fungi from phyla Ascomycota, Basidiomycota, and Mortierellomycota in AMF, but the role of non-mycorrhizal fungi associated with AMF remains unclear. Previous studies showed that AMF selectively alter the composition of the mycorrhizosphere's microorganisms, promoting the growth of beneficial microorganisms and activating those that are antagonistic to soilborne pathogenic bacteria (Dey and Ghosh, 2022; Pérez-de-Luque et al., 2017).

Furthermore, our AMF inoculum is also a complex community of mycorrhizal fungi that belonged to genera *Acaulospora*, *Claroideoglossum*, *Funnelformis*, *Rhizophagus* and *Glomus*, which are known for their growth promotion capacity (Antunes et al., 2009; Basiru and Hijri, 2022; Begum et al., 2019) and can be found associated with many plant families, including the chrysanthemum family *Asteraceae* (Sokornova et al., 2022).

Notably, from the molecular characterization, we were only able to track back taxa from an unidentified genus from the *Glomeromycetes* class and *Paraglomus*, and we could not assign species with the same accuracy as the morphological characterization. There is currently no consensus on the best rRNA gene region as phylogenetic marker for environmental sequencing of AMF (Delavaux et al., 2022). This is mainly because the AMF reference database are based in different phylogenetic markers. In this work, we focused on the impact of AMF and combined morphological and molecular characterization of AMF. Without a solid comprehension of morphology, current research on the genetics of AMF is limited (Stürmer et al., 2021). Therefore, our method involved applying an AMF inoculum (composed of fungal spores, mycelium, and soil) along with its associated microbial communities and metabolites, which resulted in a complex and diverse community of beneficial microbes (Bianciotto and Bonfante, 2002).

The plant biomass response to AMF inoculation showed cultivar-specific effects, with mainly neutral or positive responses. For instance, Chic 45 inoculated with AMF exhibited significantly higher root biomass, increasing 40 % compared to the control. Similarly, Chic

Cream showed a significant increase in root biomass of 79 % compared to the control. Interestingly, the cultivar Chic Cream showed a significant increase in root biomass after both single bacterium SMF006 strain, and AMFc inoculation.

Our results demonstrate that some cultivars are more effective than others in recruiting PGPM. Recent studies have shown that AMFc can increase plant biomass and nutrient uptake (Pellegriano et al., 2022), confirming that their effects are mainly context-dependent and host-specific (Emmett et al., 2021; van der Heyde et al., 2017). However, our understanding of the extensive physiological and genetic diversity within and between species of AMF and their associated microbiome remains scarce. To advance our knowledge, it is necessary to do comprehensive research on diverse AMF species and isolates, as well as the microbes that accompany them, both separately and in different combinations. This will help us evaluate their capacity to colonize and benefit a variety of plant hosts when used as inoculants (Giovannini et al., 2020).

The wild chrysanthemum and trap host plant millet showed AMF colonization rates of 75 % and 60 %, respectively. In contrast, we observed low root colonization (<10 %) and only the initial stage of hyphal formation in commercial chrysanthemum cultivars. In this study, we focused solely on the early stage of chrysanthemum development from cuttings, which spans a period of 22 days. This duration corresponds to the time required for plantlet production in nurseries, prior to their transplantation to the field or greenhouse for production purposes. The 22 days is a relatively short time to observe full root colonization. Nevertheless, the modern cultivars are the result of a long breeding process that might have interfered with the capacity of these cultivars to form mycorrhiza. To accurately represent all AMF present in a community, it is crucial to provide sufficient time for both slow and fast colonizing isolates to colonize (Hart and Reader, 2002).

The differential impact of AMFc inoculation on the soil microbiome of various chrysanthemum cultivars was markedly different from that of bacterial isolates. The AMFc inoculum elicited a significant shift in microbiome profiles compared to the control treatment, and the inoculated communities showed greater similarity to each other than to their corresponding controls. As a result, the introduction of a complex community (i.e., AMFc inoculum) reduced the cultivar capacity to govern the rhizosphere microbiome assembly. PGPM inoculations follow a framework similar to microbial invasions (Liu et al., 2022), where microbial inoculants can favor or outcompete native microbial populations, leading to changes in species diversity and community composition (Bannar-Martin et al., 2018). Consequently, the invaders can also reshape the functionality of resident soil communities (Amor et al., 2020; Mallon et al., 2018). By inoculating our isolates into an already living and complex soil, we could better observe the response of those communities to the 'invasive' plant-beneficial microbes and explore the effects of invasions with single and a community of microbes. Our results revealed that inoculation with more complex communities led to stronger shifts in the plant rhizosphere microbiome.

## 5. Conclusion

The development of effective microbial inoculants for plant growth promotion is hindered by a lack of understanding of how the native soil community responds to PGPM inoculation and how plant genetic variability affects the recruitment of PGPM. This study addressed these issues by collecting microbes from a wild relative of chrysanthemum and evaluating their potential plant-growth promotion in different cultivars of the target plant cultivated in a complex living soil substrate. Results revealed that cultivar preference governs the plant response to the inoculation of growth-promoting microbes, but it gets weaker when a complex community of beneficial microbes is inoculated. In summary, inoculation with a complex community of AMF and its accompanying microbiome (AMFc) led to a significant shift in microbiome profiles in the rhizosphere of the cultivars compared to the control treatment. We,

therefore, suggest that increasing the complex community of beneficial microbes can lead to stronger responses in plant growth promotion, especially in living soils with an already established microbial community.

## CRediT authorship contribution statement

**Cristina Rotoni:** Conceptualization, Formal analysis, Investigation, Methodology, Writing – original draft. **Marcio F.A. Leite:** Conceptualization, Formal analysis, Investigation, Methodology, Writing – original draft. **Lina C. Wong:** Methodology, Validation. **Catia Pinto:** Methodology. **Sidney L. Stürmer:** Data curation, Investigation, Methodology, Validation. **Agata Pijl:** Investigation, Methodology. **Eiko E. Kuramae:** Conceptualization, Funding acquisition, Resources, Supervision, Writing – review & editing.

## Declaration of competing interest

The authors declare no competing interests.

## Data availability

The raw sequences from amplicon sequencing of 16S rRNA, ITS region, and AMF were deposited in the European Nucleotide Archive (ENA; <https://www.ebi.ac.uk/ena>) under the accession number PROJ-ECT PRJEB62845.

## Acknowledgements

We thank Gregor Disveld for the greenhouse advice, Dr. Adriana Silveira for the Plant Growth-Promoting traits advice, Dr. Heitor Cantarella and Dr. Kesia Lourenço for the nutrient analysis at the Agronomical Institute of Campinas—IAC (Brazil). We thank Koppert Biological Systems BV for project support and Royal Van Zanten BV for providing the chrysanthemum cuttings.

## Funding

This work was supported by the Top Consortium for Knowledge and Innovation, TKI Agri & Food (TU 17008).

## Declarations

Ethics approval was not required for this study.

## Consent for publication

Not applicable.

## Appendix A. Supplementary data

Supplementary data to this article can be found online at <https://doi.org/10.1016/j.apsoil.2024.105347>.

## References

- Abera, S., Shimels, M., Tessema, T., Raaijmakers, J.M., Dini-Andreote, F., 2022. Back to the roots: defining the core microbiome of *Sorghum bicolor* in agricultural field soils from the centre of origin. *FEMS Microbiol. Ecol.* 98, fiac136. <https://doi.org/10.1093/femsec/fiac136>.
- Albelda Berenguer, M., Monachon, M., Joseph, E., 2019. Siderophores: from natural roles to potential applications. In: *Advances in Applied Microbiology*. <https://doi.org/10.1016/bs.aambs.2018.12.001>.
- Amor, D.R., Ratzke, C., Gore, J., 2020. Transient invaders can induce shifts between alternative stable states of microbial communities. *Science. Advances* 6, eaay8676. <https://doi.org/10.1126/sciadv.aay8676>.
- Antunes, P.M., Koch, A.M., Dunfield, K.E., Hart, M.M., Downing, A., Rillig, M.C., Klironomos, J.N., 2009. Influence of commercial inoculation with *Glomus intraradices* on the structure and functioning of an AM fungal community from an

- agricultural site. *Plant and Soil* 317, 257–266. <https://doi.org/10.1007/s11104-008-9806-y>.
- Armada, E., Leite, M.F.A., Medina, A., Azcón, R., Kuramae, E.E., 2018. Native bacteria promote plant growth under drought stress condition without impacting the rhizomicrobiome. *FEMS Microbiol. Ecol.* 94, fty092. <https://doi.org/10.1093/femsec/fty092>.
- Babraham Bioinformatics - FastQC a Quality Control Tool for High Throughput Sequence Data [WWW Document]. n.d. URL. <https://www.bioinformatics.babraham.ac.uk/projects/fastqc/> (accessed 11.18.21).
- Bannar-Martin, K.H., Kremer, C.T., Ernest, S.K.M., Leibold, M.A., Auge, H., Chase, J., Declerck, S.A.J., Eisenhauer, N., Harpole, S., Hillebrand, H., Isbell, F., Koffel, T., Larsen, S., Narwani, A., Petermann, J.S., Roscher, C., Cabral, J.S., Supp, S.R., 2018. Integrating community assembly and biodiversity to better understand ecosystem function: the Community Assembly and the Functioning of Ecosystems (CAFE) approach. *Ecol. Lett.* 21, 167–180. <https://doi.org/10.1111/ele.12895>.
- Bardsley, C.E., Lancaster, J.D., 1960. Determination of reserve sulfur and soluble sulfates in soils. *Soil Sci. Soc. Am. J.* 24, 265–268. <https://doi.org/10.2136/sssaj1960.03615995002400040015x>.
- Basiru, S., Hijri, M., 2022. The potential applications of commercial arbuscular mycorrhizal fungal inoculants and their ecological consequences. *Microorganisms* 10, 1897. <https://doi.org/10.3390/microorganisms10101897>.
- Basu, A., Prasad, P., Das, S.N., Kalam, S., Sayyed, R.Z., Reddy, M.S., El Enshasy, H., 2021. Plant growth promoting rhizobacteria (PGPR) as green bioinoculants: recent developments, constraints, and prospects. *Sustainability* 13, 1140. <https://doi.org/10.3390/su13031140>.
- Begum, N., Qin, C., Ahanger, M.A., Raza, S., Khan, M.I., Ashraf, M., Ahmed, N., Zhang, L., 2019. Role of arbuscular mycorrhizal fungi in plant growth regulation: implications in abiotic stress tolerance. *Front. Plant Sci.* 10.
- Bianciotto, V., Bonfante, P., 2002. Arbuscular mycorrhizal fungi: a specialised niche for rhizospheric and endocellular bacteria. *Antonie Van Leeuwenhoek* 81, 365–371. <https://doi.org/10.1023/A:1020544919072>.
- Biedendieck, R., Knuutti, T., Moore, S.J., Jahn, D., 2021. The “beauty in the beast”—the multiple uses of *Priestia megaterium* in biotechnology. *Appl. Microbiol. Biotechnol.* 105, 5719–5737. <https://doi.org/10.1007/s00253-021-11424-6>.
- Bonfante, P., 2018. The future has roots in the past: the ideas and scientists that shaped mycorrhizal research. *New Phytol.* 220, 982–995. <https://doi.org/10.1111/nph.15397>.
- Bric, J.M., Bostock, R.M., Silverstone, S.E., 1991. Rapid in situ assay for indole acetic acid production by bacteria immobilized on a nitrocellulose membrane. *Appl. Environ. Microbiol.* 57, 535–538. <https://doi.org/10.1128/aem.57.2.535-538.1991>.
- Bulgarelli, R.G., Leite, M.F.A., de Hollander, M., Mazzafera, P., Andrade, S.A.L., Kuramae, E.E., 2022. Eucalypt species drive rhizosphere bacterial and fungal community assembly but soil phosphorus availability rearranges the microbiome. *Sci. Total Environ.* 836, 155667. <https://doi.org/10.1016/j.scitotenv.2022.155667>.
- Callahan, B.J., McMurdie, P.J., Rosen, M.J., Han, A.W., Johnson, A.J.A., Holmes, S.P., 2016. DADA2: high-resolution sample inference from Illumina amplicon data. *Nat. Methods* 13, 581–583. <https://doi.org/10.1038/nmeth.3869>.
- Chang, J., Shi, S., Tian, L., Leite, M.F.A., Chang, C., Ji, L., Ma, L., Tian, C., Kuramae, E.E., 2021a. Self-crossing leads to weak co-variation of the bacterial and fungal communities in the rice rhizosphere. *Microorganisms* 9, 175. <https://doi.org/10.3390/microorganisms9010175>.
- Chang, J., Sun, Y., Tian, L., Ji, L., Luo, S., Nasir, F., Kuramae, E.E., Tian, C., 2021b. The structure of rhizosphere fungal communities of wild and domesticated rice: changes in diversity and co-occurrence patterns. *Front. Microbiol.* 12. <https://doi.org/10.3389/fmicb.2021.610823>.
- Chang, J., van Veen, J.A., Tian, C., Kuramae, E.E., 2022. A review on the impact of domestication of the rhizosphere of grain crops and a perspective on the potential role of the rhizosphere microbial community for sustainable rice crop production. *Sci. Total Environ.* 842, 156706. <https://doi.org/10.1016/j.scitotenv.2022.156706>.
- Cipriano, M.A.P., Lupatini, M., Lopes-Santos, L., da Silva, M.J., Roesch, L.F.W., Destéfano, S.A.L., Freitas, S.S., Kuramae, E.E., 2016. Lettuce and rhizosphere microbiome responses to growth promoting *Pseudomonas* species under field conditions. *FEMS Microbiol. Ecol.* 92. <https://doi.org/10.1093/femsec/fiw197>.
- Clark, J.S., Nemergut, D., Seyedsnollah, B., Turner, P.J., Zhang, S., 2017. Generalized joint attribute modeling for biodiversity analysis: median-zero, multivariate, multifarious data. *Ecological monographs*. <https://doi.org/10.1002/ecm.1241>.
- Delavaux, C.S., Ramos, R.J., Sturmer, S.L., Bever, J.D., 2022. Environmental identification of arbuscular mycorrhizal fungi using the LSU rDNA gene region: an expanded database and improved pipeline. *Mycorrhiza* 32, 145–153. <https://doi.org/10.1007/s00572-022-01068-3>.
- Dey, M., Ghosh, S., 2022. Arbuscular mycorrhizae in plant immunity and crop pathogen control. *Rhizosphere* 22, 100524. <https://doi.org/10.1016/j.rhisph.2022.100524>.
- Elsisi, A., 2019. Bacterial Blight Disease Caused by *Pseudomonas cichorii* on *Chrysanthemum* in Egypt, 6, pp. 11–23.
- Emmett, B.D., Lévesque-Tremblay, V., Harrison, M.J., 2021. Conserved and reproducible bacterial communities associate with extraradical hyphae of arbuscular mycorrhizal fungi. *ISME J.* 15, 2276–2288. <https://doi.org/10.1038/s41396-021-00920-2>.
- Ferreira, E.B., Cavalcanti, P.P., Nogueira, D.A., 2014. ExpDes: an R package for ANOVA and experimental designs. *Appl. Math.* 5, 2952–2958. <https://doi.org/10.4236/am.2014.519280>.
- Gerdemann, J.W., Nicolson, T.H., 1963. Spores of mycorrhizal endogone species extracted from soil by wet sieving and decanting. *Trans. Br. Mycol. Soc.* 46, 235–244. [https://doi.org/10.1016/S0007-1536\(63\)80079-0](https://doi.org/10.1016/S0007-1536(63)80079-0).
- Giovannetti, M., Mosse, B., 1980. An evaluation of techniques for measuring vesicular arbuscular mycorrhizal infection in roots. *New Phytol.* 84, 489–500. <https://doi.org/10.1111/j.1469-8137.1980.tb04556.x>.
- Giovannetti, L., Palla, M., Agnolucci, M., Avio, L., Sbrana, C., Turrini, A., Giovannetti, M., 2020. Arbuscular mycorrhizal fungi and associated microbiota as plant biostimulants: research strategies for the selection of the best performing inocula. *Agronomy* 10, 106. <https://doi.org/10.3390/agronomy10010106>.
- Gloor, G.B., Macklaim, J.M., Pawlowsky-Glahn, V., Egozcue, J.J., 2017. Microbiome datasets are compositional: and this is not optional. *Front. Microbiol.* 0. <https://doi.org/10.3389/fmicb.2017.02224>.
- Hart, M.M., Reader, R.J., 2002. Taxonomic basis for variation in the colonization strategy of arbuscular mycorrhizal fungi. *New Phytol.* 153, 335–344. <https://doi.org/10.1046/j.0028-646X.2001.00312.x>.
- Helgason, T., Daniell, T.J., Husband, R., Fitter, A.H., Young, J.P.W., 1998. Ploughing up the wood-wide web? *Nature* 394, 431.
- Higo, M., Kang, D.-J., Isoke, K., 2019. First report of community dynamics of arbuscular mycorrhizal fungi in radiocesium degradation lands after the Fukushima-Daiichi nuclear disaster in Japan. *Sci. Rep.* 9, 8240. <https://doi.org/10.1038/s41598-019-44665-7>.
- Leite, M.F.A., Kuramae, E.E., 2020. You must choose, but choose wisely: model-based approaches for microbial community analysis. *Soil Biol. Biochem.* 151, 108042. <https://doi.org/10.1016/j.soilbio.2020.108042>.
- Leite, M.F., Pan, Y., Bloem, J., Berge, H.T., Kuramae, E.E., 2017. Organic nitrogen rearranges both structure and activity of the soil-borne microbial seedbank. *Sci. Rep.* 7, 42634. <https://doi.org/10.1038/srep42634>.
- Leite, M.F.A., Dimitrov, M.R., Freitas-Iório, R.P., de Hollander, M., Cipriano, M.A.P., Andrade, S.A.L., da Silva, A.P.D., Kuramae, E.E., 2021. Rearranging the sugarcane holobiont via plant growth-promoting bacteria and nitrogen input. *Sci. Total Environ.* 800, 149493. <https://doi.org/10.1016/j.scitotenv.2021.149493>.
- Li, S., Li, G., Huang, X., Chen, Y., Lv, C., Bai, L., Zhang, K., He, H., Dai, J., 2023. Cultivar-specific response of rhizosphere bacterial community to uptake of cadmium and mineral elements in rice (*Oryza sativa* L.). *Ecotoxicol. Environ. Saf.* 249, 114403. <https://doi.org/10.1016/j.ecoenv.2022.114403>.
- Liu, X., Le Roux, X., Salles, J.F., 2022. The legacy of microbial inoculants in agroecosystems and potential for tackling climate change challenges. *iScience* 25, 103821. <https://doi.org/10.1016/j.isci.2022.103821>.
- Lumini, E., Orgiazzi, A., Borriello, R., Bonfante, P., Bianciotto, V., 2010. Disclosing arbuscular mycorrhizal fungal biodiversity in soil through a land-use gradient using a pyrosequencing approach. *Environ. Microbiol.* 12, 2165–2179. <https://doi.org/10.1111/j.1462-2920.2009.02099.x>.
- Ma, S., Xia, X., Li, Y., Sun, L., Liu, Yue, Liu, Yuanyuan, Wang, X., Shi, R., Chang, J., Zhao, P., Xia, Q., 2017. Increasing the yield of middle silk gland expression system through transgenic knock-down of endogenous sericin-1. *Mol. Genet. Genomics* 292, 823–831. <https://doi.org/10.1007/s00438-017-1311-7>.
- Mallon, C.A., Le Roux, X., van Doorn, G.S., Dini-Andreote, F., Poly, F., Salles, J.F., 2018. The impact of failure: unsuccessful bacterial invasions steer the soil microbial community away from the invader's niche. *ISME J.* 12, 728–741. <https://doi.org/10.1038/s41396-017-0003-y>.
- Martin, M., 2011. Cutadapt removes adapter sequences from high-throughput sequencing reads. *EMBnet journal* 17, 10–12. <https://doi.org/10.14806/ej.17.1.200>.
- Mulvaney, R.L., 1996. Nitrogen—inorganic forms. In: *Methods of Soil Analysis*. John Wiley & Sons, Ltd, pp. 1123–1184. <https://doi.org/10.2136/sssabookser5.3.c38>.
- Naamala, J., Smith, D.L., 2020. Relevance of plant growth promoting microorganisms and their derived compounds, in the face of climate change. *Agronomy* 10, 1179. <https://doi.org/10.3390/agronomy10081179>.
- Nascimento, F.X., Hernández, A.G., Glick, B.R., Rossi, M.J., 2020. Plant growth-promoting activities and genomic analysis of the stress-resistant *Bacillus megaterium* STB1, a bacterium of agricultural and biotechnological interest. *Biotechnol. Rep. (Amst.)* 25, e00406. <https://doi.org/10.1016/j.btre.2019.e00406>.
- Nautiyal, C.S., 1999. An efficient microbiological growth medium for screening phosphate solubilizing microorganisms. *FEMS Microbiol. Lett.* 170, 265–270. <https://doi.org/10.1111/j.1574-6968.1999.tb13383.x>.
- Nilsson, R.H., Larsson, K.-H., Taylor, A.F.S., Bengtsson-Palme, J., Jeppesen, T.S., Schigel, D., Kennedy, P., Picard, K., Glöckner, F.O., Tedersoo, L., Saar, I., Kõljalg, U., Abarenkov, K., 2019. The UNITE database for molecular identification of fungi: handling dark taxa and parallel taxonomic classifications. *Nucleic Acids Res.* 47, D259–D264. <https://doi.org/10.1093/nar/gky1022>.
- Oksanen, J., Blanchet, F.G., Kindt, R., Legendre, P., Minchin, P., O'Hara, R., Simpson, G., Solymos, P., Stevens, M., Wagner, H., 2012. *Vegan: Community Ecology Package (R package version 2.0-2)*.
- Öpik, M., Vanatoa, A., Vanatoa, E., Moora, M., Davison, J., Kalwij, J.M., Reier, Ü., Zobel, M., 2010. The online database MaarjAM reveals global and ecosystemic distribution patterns in arbuscular mycorrhizal fungi (Glomeromycota). *New Phytol.* 188, 223–241. <https://doi.org/10.1111/j.1469-8137.2010.03334.x>.
- Ortiz-Castro, R., Valencia-Cantero, E., López-Bucio, J., 2008. Plant growth promotion by *Bacillus megaterium* involves cytokinin signaling. *Plant Signal. Behav.* 3, 263–265. <https://doi.org/10.4161/psb.3.4.5204>.
- Oyserman, B.O., Cordovez, V., Flores, S.S., Leite, M.F.A., Nijveen, H., Medema, M.H., Raaijmakers, J.M., 2021. Extracting the GEMs: endotype, environment, and microbiome interactions shaping host phenotypes. *Front. Microbiol.* 11, 3444. <https://doi.org/10.3389/fmicb.2020.574053>.
- Parnell, J.J., Berka, R., Young, H.A., Sturino, J.M., Kang, Y., Barnhart, D.M., DiLoro, M.V., 2016. From the lab to the farm: an industrial perspective of plant beneficial microorganisms. *Front. Plant Sci.* 7.
- Passera, A., Compant, S., Casati, P., Maturo, M.G., Battelli, G., Quaglino, F., Antonielli, L., Salerno, D., Brasca, M., Toffolatti, S.L., Mantegazza, F., Delledonne, M., Mitter, B., 2019. Not just a pathogen? Description of a plant-beneficial *Pseudomonas syringae* strain. *Front. Microbiol.* 10.

- Pellegrino, E., Nuti, M., Ercoli, L., 2022. Multiple arbuscular mycorrhizal fungal consortia enhance yield and fatty acids of *Medicago sativa*: a two-year field study on agronomic traits and tracing of fungal persistence. *Front. Plant Sci.* 13, 814401. <https://doi.org/10.3389/fpls.2022.814401>.
- Pérez-de-Luque, A., Tille, S., Johnson, I., Pascual-Pardo, D., Ton, J., Cameron, D.D., 2017. The interactive effects of arbuscular mycorrhiza and plant growth-promoting rhizobacteria synergistically enhance host plant defences against pathogens. *Sci. Rep.* 7, 16409. <https://doi.org/10.1038/s41598-017-16697-4>.
- Quast, C., Pruesse, E., Yilmaz, P., Gerken, J., Schweer, T., Yarza, P., Peplies, J., Glöckner, F.O., 2013. The SILVA ribosomal RNA gene database project: improved data processing and web-based tools. *Nucleic Acids Res.* 41, D590–D596. <https://doi.org/10.1093/nar/gks1219>.
- Raij, B., Cantarella, H., Quaggio, J., Prochnow, L., 2009. Ion Exchange Resin for Assessing Phosphorus Availability in Soils.
- Roesti, D., Ineichen, K., Braissant, O., Redecker, D., Wiemken, A., Aragno, M., 2005. Bacteria associated with spores of the arbuscular mycorrhizal fungi *Glomus geosporum* and *Glomus constrictum*. *Appl. Environ. Microbiol.* 71, 6673–6679. <https://doi.org/10.1128/AEM.71.11.6673-6679.2005>.
- Rojas-Tapias, D.F., Bonilla, R., Dussán, J., 2014. Effect of inoculation and co-inoculation of *Acinetobacter* sp. RG30 and *Pseudomonas putida* GN04 on growth, fitness, and copper accumulation of maize (*Zea mays*). *Water Air Soil Pollut.* 225, 2232. <https://doi.org/10.1007/s11270-014-2232-2>.
- Rotoni, C., Leite, M.F.A., Pijl, A., Kuramae, E.E., 2022. Rhizosphere microbiome response to host genetic variability: a trade-off between bacterial and fungal community assembly. *FEMS Microbiol. Ecol.* 98, fiac061. <https://doi.org/10.1093/femsec/fiac061>.
- Schlemper, T.R., Leite, M.F.A., Lucheta, A.R., Shimels, M., Bouwmeester, H.J., Veen, V., A, J., Kuramae, E.E., 2017. Rhizobacterial community structure differences among sorghum cultivars in different growth stages and soils. *FEMS Microbiol. Ecol.* 93. <https://doi.org/10.1093/femsec/fix096>.
- Schlemper, T.R., Dimitrov, M.R., Gutierrez, F.A.O.S., Veen, J.A. van, Silveira, A.P.D., Kuramae, E.E., 2018. Effect of *Burkholderia tropica* and *Herbaspirillum frisingense* strains on sorghum growth is plant genotype dependent. *PeerJ* 6, e5346. <https://doi.org/10.7717/peerj.5346>.
- Schwyn, B., Neillands, J.B., 1987. Universal chemical assay for the detection and determination of siderophores. *Anal. Biochem.* 160, 47–56. [https://doi.org/10.1016/0003-2697\(87\)90612-9](https://doi.org/10.1016/0003-2697(87)90612-9).
- Shoemaker, H.E., McLean, E.O., Pratt, P.F., 1961. Buffer methods for determining lime requirement of soils with appreciable amounts of extractable aluminum. *Soil Sci. Soc. Am. J.* 25, 274–277. <https://doi.org/10.2136/sssaj1961.03615995002500040014x>.
- Sokornova, S., Malygin, D., Terentev, A., Dolzhenko, V., 2022. Arbuscular mycorrhiza symbiosis as a factor of *Asteraceae* species invasion. *Agronomy* 12, 3214. <https://doi.org/10.3390/agronomy12123214>.
- Stürmer, S.L., Bever, J.D., Schultz, P.A., Bentivenga, S.P., 2021. Celebrating INVAM: 35 years of the largest living culture collection of arbuscular mycorrhizal fungi. *Mycorrhiza* 31, 117–126. <https://doi.org/10.1007/s00572-020-01008-z>.
- Stutz, J.C., Morton, J.B., 1996. Successive pot cultures reveal high species richness of arbuscular endomycorrhizal fungi in arid ecosystems. *Can. J. Bot.* 74, 1883–1889. <https://doi.org/10.1139/b96-225>.
- Team, R.C., 2019. R: A Language and Environment for Statistical Computing (Vienna, Austria).
- van der Heyde, M., Ohsowski, B., Abbott, L.K., Hart, M., 2017. Arbuscular mycorrhizal fungus responses to disturbance are context-dependent. *Mycorrhiza* 27, 431–440. <https://doi.org/10.1007/s00572-016-0759-3>.
- van Raij, B., de Andrade, J.C., Cantarella, H., Quaggio, J.A., 2001. Análise química para avaliação da fertilidade de solos tropicais. Instituto Agronômico.
- Vierheilig, H., Coughlan, A.P., Wyss, U., Piché, Y., 1998. Ink and vinegar, a simple staining technique for arbuscular mycorrhizal fungi. *Appl. Environ. Microbiol.* 64, 5004–5007.
- Wang, Q., Garrity, G.M., Tiedje, J.M., Cole, J.R., 2007. Naïve Bayesian classifier for rapid assignment of rRNA sequences into the new bacterial taxonomy. *Appl. Environ. Microbiol.* 73, 5261. <https://doi.org/10.1128/AEM.00062-07>.
- Wang, Z., Xu, Z., Chen, Z., Kowalchuk, G.A., Fu, X., Kuramae, E.E., 2021. Microbial inoculants modulate growth traits, nutrients acquisition and bioactive compounds accumulation of *Cyclocarya paliurus* (Batal.) Iljinskaja under degraded field condition. *For. Ecol. Manage.* 482, 118897. <https://doi.org/10.1016/j.foreco.2020.118897>.
- Wang, Z., Chen, Z., Leite, M.F.A., Xu, Z., Lin, Q., Kowalchuk, G.A., Fu, X., Kuramae, E.E., 2022. Effects of probiotic consortia on plant metabolites are associated with soil indigenous microbiota and fertilization regimes. *Ind. Crop. Prod.* 185, 115138. <https://doi.org/10.1016/j.indcrop.2022.115138>.
- Wickham, H., 2009. ggplot2: Elegant Graphics for Data Analysis. Springer, New York, NY. <https://doi.org/10.1007/978-0-387-98141-3>.
- Zhou, Y., Wang, Y., Zhu, X., Liu, R., Xiang, P., Chen, J., Liu, X., Duan, Y., Chen, L., 2017. Management of the soybean cyst nematode *Heterodera glycines* with combinations of different rhizobacterial strains on soybean. *PLoS One* 12, e0182654. <https://doi.org/10.1371/journal.pone.0182654>.